

Hyperon production in quasielastic $\bar{\nu}_\tau$ -nucleon scattering

A. Fatima,¹ M. Sajjad Athar,^{1,*} and S. K. Singh¹

¹*Department of Physics, Aligarh Muslim University, Aligarh-202002, India*

The theoretical results for the total cross sections and polarization components of the τ^+ lepton produced in the charged current induced $|\Delta S| = 1$ quasielastic $\bar{\nu}_\tau - N$ scattering leading to hyperons (Λ, Σ) have been presented assuming T invariance. The theoretical uncertainties arising due to the use of different vector, axial vector and pseudoscalar form factors as well as the effect of SU(3) symmetry breaking have been studied. We have also presented, for the first time, a comparison of the total cross sections for the production of e, μ, τ leptons to facilitate the implications of lepton flavor universality (LFU) in the $|\Delta S| = 1$ quasielastic reactions induced by the antineutrinos of all flavors *i.e.*, ν_l ; $l = e, \mu, \tau$.

PACS numbers: 12.15.-y, 13.15.+g, 13.88.+e

I. INTRODUCTION

The τ neutrinos (ν_τ) were experimentally observed for the first time by the DONUT collaboration [1, 2] by observing the τ^- leptons produced through the charged current scattering of ν_τ on the nucleons in the reaction, $\nu_\tau + N \rightarrow \tau^- + X$, where $N = n$ or p , and X represents hadron(s) in the final state. Since then, a few τ^- production events have been observed by the OPERA collaboration at CERN [3–5] using accelerator neutrinos and by the SuperKamiokande [6, 7] as well as the IceCUBE [8] collaborations using the atmospheric neutrinos where the ν_τ s are assumed to be produced through the $\nu_\mu \rightarrow \nu_\tau$ oscillation. Since these experiments have observed very few events of the τ lepton production, new experiments for producing larger number of τ leptons have been proposed by the SHiP [9–11], DsTau [12], DUNE [13–15] and FASER ν [16] collaborations in which the number of τ lepton events are expected to reach a few hundreds during the running time of 3–5 years of the experiment. The results from these experiments would provide the desired data with reasonable statistics on the total and differential scattering cross sections as well as on the polarization components of the τ lepton, which would enable a reliable study of the various aspects and properties of ν_τ and τ leptons.

The τ lepton production in $\nu_\tau - N$ scattering has a threshold of 3.5 GeV in the charged current induced quasielastic (CCQE) reactions *i.e.*, $\nu_\tau(\bar{\nu}_\tau) + N \rightarrow \tau^-(\tau^+) + N'$ ($N, N' = n$ or p). As the energy increases, the production of the τ leptons is accompanied with the inelastic and deep inelastic production of hadrons. In the energy region of ν_τ ($\bar{\nu}_\tau$) experiments, where the energy of the produced τ lepton is not too large compared to its rest mass $m_\tau = 1.776$ GeV, the τ leptons would not be completely longitudinally polarized, and would also have transverse component of the polarization [17–24]. Moreover, any presence of the polarization component perpendicular to the reaction plane would provide information about the T noninvariance in $\nu_\tau - N$ interactions [25–28]. The polarization state of the τ lepton affects the total and differential cross sections and is, therefore, an important observable in the study of $\nu_\tau - N$ interactions. Thus, it is highly desirable that a comprehensive study of the τ polarization along with the cross sections be made in the quasielastic, inelastic and deep inelastic reactions induced by ν_τ and $\bar{\nu}_\tau$ on nucleons in order to understand the $\nu_\tau - N$ interactions.

In the case of Standard Model (SM) of particle physics, all the leptons interact with each other through the purely leptonic processes and with the quarks through the various semileptonic processes, having the same strength for each leptonic flavor. This is called the lepton flavor universality (LFU) and is an essential feature of the SM.

The validity of LFU has been experimentally studied in the purely leptonic decays of μ, τ leptons as well as in the various semileptonic decays of mesons and baryons. The LFU seems to work quite well in the case of purely leptonic decays of μ and τ leptons and W boson [29]. In the case of semileptonic decays of mesons and baryons like K, D, D_s^*, Λ and Λ_c , etc., involving quark transitions between medium heavy and light quarks *i.e.*, $s \rightarrow ul\bar{\nu}_l$, $s \rightarrow dl\bar{l}$, $c \rightarrow sl\bar{\nu}_l$, $c \rightarrow dl\bar{\nu}_l$, etc., the available experimental results are in agreement with the prediction of SM within statistical uncertainties and no evidence of LFU violation (LFUV) has been reported [30–36]. However, the recent indications of LFUV in semileptonic decays in the heavy quark sector involving transitions like $b \rightarrow sl\bar{l}$ and $b \rightarrow cl\bar{\nu}_l$ at BaBar, LHCb, BESIII and Belle collaborations [37–42] have generated great interest in studying

*Electronic address: sajathar@gmail.com

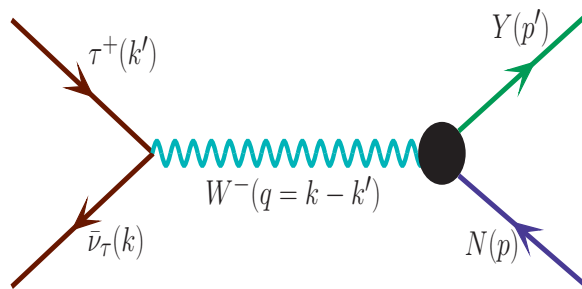


FIG. 1: Feynman diagram for the process $\bar{\nu}_\tau(k) + N(p) \rightarrow \tau^+(k') + Y(p')$, where $N = p, n$; $Y = \Lambda, \Sigma^0, \Sigma^-$ and the quantities in the bracket represent four momenta of the corresponding particles.

the origins of LFUV. Further hints for the LFUV [43, 44] have been inferred from the recent measurements of the anomalous magnetic moment ($g - 2$) of the muons, at the Fermilab [45], as well as the anomalies reported in the recent measurements of the Cabibbo angle [46] and production of lepton pairs through the process of $q\bar{q} \rightarrow l\bar{l}$ ($l = e$ and μ) in pp collisions at CERN [47]. In the case of $b \rightarrow s\bar{l}l$ decays, LHCb [39] collaboration has reported the ratio of the branching fractions in $l = \mu$ mode to $l = e$ mode to be 2.6σ lower than the SM prediction. While in the case of $b \rightarrow c\bar{l}l$ decays, all the three collaborations [37] have reported the ratio of the branching fraction in $l = \tau$ mode to $l = \mu$ mode, which challenge LFU at the level of four standard deviation. This has led to extensive theoretical work in constructing the models of new physics (NP) going beyond the standard model (BSM) to explain these experimental results on LFUV in the b quark sector [48–50]. In view of these developments in b quark sector, it is natural to apply these theoretical models [48–50] in the medium heavy quark sector involving c and s quarks decays like $c \rightarrow s\bar{l}l$, $c \rightarrow d\bar{l}l$, $s \rightarrow u\bar{l}l$, $s \rightarrow d\bar{l}l$ and critically study the LFUV effects and search for them experimentally [51–54]. While these studies are being pursued with some interest, the need for further efforts in this direction has been emphasized recently [34].

Notwithstanding the above efforts in the study of LFUV in the semileptonic decays, there have been almost no study of LFUV effects in the (anti)neutrino-nucleon scattering. The only exception is comparative study of the quasielastic $\nu_e(\bar{\nu}_e)$ -nucleon/nucleus and $\nu_\mu(\bar{\nu}_\mu)$ -nucleon/nucleus scattering and analyzing the differences in the cross sections of these processes arising due to the lepton mass and the radiative corrections and the contributions due to the pseudoscalar and second class current form factors [55, 56]. A comparison with the experimental results would give information about the presence or absence of any LFUV effects, however, the present results on the cross sections in the neutrino energy region of a few GeV are not precise enough to conclude about the presence of LFUV effects. Such studies of LFUV effects in the (anti)neutrino scattering with $\nu_l(\bar{\nu}_l)$; ($l = e, \mu, \tau$) in the strange, charm, bottom and top quark sectors have not been done. With the aim of exploring the presence of such effects in the strangeness sector, we have studied in some detail the quasielastic scattering process of $\bar{\nu}_l + N \rightarrow l^+ + \Lambda(\Sigma)$; ($l = e, \mu, \tau$) corresponding to $u \rightarrow s$ transition.

In this work, we report on the results of the theoretical calculations within the ambit of the SM with implicit lepton flavor universality for the total cross section, differential cross section and the τ lepton polarization in the reaction $\bar{\nu}_\tau + p \rightarrow \tau^+ + \Lambda(\Sigma)$, using various parameterizations for the vector and axial vector form factors using SU(3) symmetry. The uncertainties in the numerical values of these observables due to the use of different parameterizations of the form factors are discussed. We have also studied the effect of SU(3) symmetry violation using the various weak form factors which have been used to study the SU(3) symmetry violating effects in the semileptonic hyperon decays of Λ and Σ [57, 58] and have discussed the uncertainties associated with SU(3) violations. Any deviation of the experimental results on the cross sections and τ polarization to be obtained in future will be a signal of LFUV. The results presented here would facilitate the study of LFUV effects in $\bar{\nu}_l$ ($l = e, \mu, \tau$) induced processes in the strangeness sector corresponding to $u \rightarrow s$ transition and compliment such LFUV studies in the semileptonic decays of strange particles [59].

In section II, we present the formalism for calculating the differential and total scattering cross sections and using them the polarization observables of the τ lepton produced in the quasielastic $|\Delta S| = 1$ scattering processes have been discussed in section-III. In section IV A, we present and discuss the numerical results obtained for the differential cross section and polarization observables of the τ lepton and study the dependence of the different parameteric forms of the vector and axial vector form factors as well as the effect of SU(3) symmetry breaking on these observables. Similar effects are studied in the case of total cross sections and average polarizations in section IV B. Further, we have also studied the lepton flavor universality in the case of $e - \mu$ and $e - \mu - \tau$ sectors in the total cross sections and

the numerical results are presented for the ratios $R_1 = \frac{\sigma(\bar{\nu}_\mu + p \rightarrow \mu^+ + \Lambda)}{\sigma(\bar{\nu}_e + p \rightarrow e^+ + \Lambda)}$ and $R_2 = \frac{2\sigma(\bar{\nu}_\tau + p \rightarrow \tau^+ + \Lambda)}{\sigma(\bar{\nu}_\mu + p \rightarrow \mu^+ + \Lambda) + \sigma(\bar{\nu}_e + p \rightarrow e^+ + \Lambda)}$, in Section IV C. Section V summarizes the results and conclude our findings.

II. FORMALISM

A. Matrix element and weak form factors

1. Matrix element

The transition matrix element for the quasielastic hyperon production processes depicted in Fig. 1, given by

$$\bar{\nu}_\tau(k) + N(p) \longrightarrow \tau^+(k') + Y(p'), \quad N = p, n; \quad Y = \Lambda, \Sigma^0, \Sigma^-, \quad (1)$$

is written as

$$\mathcal{M} = \frac{G_F}{\sqrt{2}} \sin \theta_c l^\mu J_\mu, \quad (2)$$

where the quantities in the brackets of Eq. (1) represent the four momenta of the respective particles, G_F is the Fermi coupling constant and θ_c ($= 13.1^\circ$) is the Cabibbo mixing angle. The leptonic current l^μ is given by

$$l^\mu = \bar{u}(k') \gamma^\mu (1 + \gamma_5) u(k). \quad (3)$$

The hadronic current J_μ is expressed as:

$$J_\mu = \bar{u}(p') \Gamma_\mu u(p) \quad (4)$$

with

$$\Gamma_\mu = V_\mu - A_\mu. \quad (5)$$

The vector (V_μ) and the axial vector (A_μ) currents are given by [25, 26]:

$$\langle Y(p') | V_\mu | N(p) \rangle = \bar{u}(p') \left[\gamma_\mu f_1^{NY}(Q^2) + i \sigma_{\mu\nu} \frac{q^\nu}{M + M_Y} f_2^{NY}(Q^2) + \frac{2 q_\mu}{M + M_Y} f_3^{NY}(Q^2) \right] u(p), \quad (6)$$

$$\langle Y(p') | A_\mu | N(p) \rangle = \bar{u}(p') \left[\gamma_\mu \gamma_5 g_1^{NY}(Q^2) + i \sigma_{\mu\nu} \frac{q^\nu}{M + M_Y} \gamma_5 g_2^{NY}(Q^2) + \frac{2 q_\mu}{M + M_Y} g_3^{NY}(Q^2) \gamma_5 \right] u(p), \quad (7)$$

where M and M_Y are the masses of the initial nucleon and the final hyperon. $q (= k - k' = p' - p)$ is the four momentum transfer with $Q^2 = -q^2, Q^2 \geq 0$. $f_1^{NY}(Q^2)$, $f_2^{NY}(Q^2)$ and $f_3^{NY}(Q^2)$ are the $N - Y$ transition vector, weak magnetic and induced scalar form factors and $g_1^{NY}(Q^2)$, $g_2^{NY}(Q^2)$ and $g_3^{NY}(Q^2)$ are the axial vector, induced tensor (or weak electric) and induced pseudoscalar form factors, respectively.

2. Weak transition form factors

The weak vector and axial vector form factors are determined using the following assumptions, which are consistent with the constraints due to the symmetry properties of the weak hadronic currents [60–62]:

- (a) T invariance implies that all the vector ($f_i^{NY}(Q^2)$; $i = 1 - 3$) and axial vector ($g_i^{NY}(Q^2)$; $i = 1 - 3$) form factors are real.
- (b) The hypothesis that the charged weak vector currents and its conjugate along with the isovector part of the electromagnetic current form an isotriplet implies that the weak vector form factors $f_1^{NY}(Q^2)$ and $f_2^{NY}(Q^2)$ are related to the isovector electromagnetic form factors of the nucleon. The hypothesis ensures conservation of vector current (CVC) in the weak sector.
- (c) The hypothesis of CVC of the weak vector currents implies that $f_3(Q^2) = 0$.

- (d) The principle of G-invariance implies the second class current form factors to be zero, *i.e.*, $f_3^{NY}(Q^2) = 0$ and $g_2^{NY}(Q^2) = 0$.
- (e) The hypothesis of partially conserved axial vector current (PCAC) relates the pseudoscalar form factor ($g_3^{NY}(Q^2)$) to the axial vector form factor ($g_1^{NY}(Q^2)$), through the Goldberger-Treiman (GT) relation.
- (f) The assumption of SU(3) symmetry of the weak hadronic currents implies that the vector and axial vector currents transform as an octet under the SU(3) group of transformations.

The determination of all the weak form factors is based on the symmetry properties discussed above, and the details are given in Ref. [25, 26]. The explicit expressions of the vector and axial vector form factors for the different $N - Y$ transitions, assuming the SU(3) symmetry are given in Section II A 3, while the effects of SU(3) symmetry breaking on these form factors are discussed in Section II A 4.

3. Form factors with SU(3) symmetry

The weak vector and the axial vector currents corresponding to the $\Delta S = 1$ currents whose matrix elements are defined between the initial ($|N\rangle$) and final ($|Y\rangle$) states in Eq. (1) are assumed to belong to the octet representation of the SU(3). Since $|N\rangle$ and $|Y\rangle$ also belong to the octet representation under SU(3), each of these form factors are described in terms of the functions $D(Q^2)$ and $F(Q^2)$ corresponding to the symmetric (S) and antisymmetric (A) couplings and the SU(3) Clebsch-Gordan coefficients. Explicitly, the form factors can be expressed as (for details, see Ref. [26]):

$$\begin{aligned} f_i(Q^2) &= aF_i^V(Q^2) + bD_i^V(Q^2) \\ g_i(Q^2) &= aF_i^A(Q^2) + bD_i^A(Q^2) \quad i = 1, 2, 3 \end{aligned} \quad (8)$$

The Clebsch-Gordan coefficients a and b are calculated for each $N - Y$ transitions and are given in Table I.

Transitions	a	b
$p \rightarrow \Lambda$	$-\sqrt{\frac{3}{2}}$	$-\frac{1}{\sqrt{6}}$
$p \rightarrow \Sigma^0$	$-\frac{1}{\sqrt{2}}$	$\frac{1}{\sqrt{2}}$
$n \rightarrow \Sigma^-$	-1	1

TABLE I: Values of the coefficients a and b given in Eqs. (8)–(9).

From Table I, we see that the SU(3) symmetry predicts a relation between the vector and axial vector form factors for the transitions $p \rightarrow \Sigma^0$ and $n \rightarrow \Sigma^-$, which implies that

$$\left[\frac{d\sigma}{dQ^2} \right]_{p \rightarrow \Sigma^0} = \frac{1}{2} \left[\frac{d\sigma}{dQ^2} \right]_{n \rightarrow \Sigma^-}, \quad (10)$$

and

$$[P_{L,P}]_{p \rightarrow \Sigma^0} = [P_{L,P}]_{n \rightarrow \Sigma^-}. \quad (11)$$

(i) Vector form factors:

In the case of vector form factors, the functions $D_i^V(Q^2)$ and $F_i^V(Q^2)$ are determined in terms of the nucleon electromagnetic form factors $f_i^{n,p}(Q^2)$; ($i = 1, 2$), following the same method as discussed above (Eq. (8)) in the case of electromagnetic interactions, *i.e.*

$$D_i^V(Q^2) = -\frac{3}{2}f_i^n(Q^2) \quad i = 1, 2 \quad (12)$$

$$F_i^V(Q^2) = f_i^p(Q^2) + \frac{1}{2}f_i^n(Q^2) \quad i = 1, 2 \quad (13)$$

Using the expressions of $D_i^V(Q^2)$ and $F_i^V(Q^2)$ obtained above and the values of the coefficients a and b from Table I, the vector form factors $f_{1,2}^{NY}(Q^2)$ are expressed in terms of the nucleon electromagnetic form factors as:

$$f_{1,2}^{p\Lambda}(Q^2) = -\sqrt{\frac{3}{2}}f_{1,2}^p(Q^2), \quad (14)$$

$$f_{1,2}^{n\Sigma^-}(Q^2) = -[f_{1,2}^p(Q^2) + 2f_{1,2}^n(Q^2)], \quad (15)$$

$$f_{1,2}^{p\Sigma^0}(Q^2) = -\frac{1}{\sqrt{2}} [f_{1,2}^p(Q^2) + 2f_{1,2}^n(Q^2)]. \quad (16)$$

The electromagnetic nucleon form factors, in turn, are expressed in the terms of the Sachs' electric ($G_E(Q^2)$) and magnetic ($G_M(Q^2)$) form factors of the nucleons, for which various parameterizations are available in the literature [63–70]. For the numerical calculations, we have used the parameterization given by Bradford *et al.* (BBBA05) [63] unless stated otherwise.

(ii) **Axial vector form factors:**

We express $g_1^{NY}(Q^2)$ in terms of $g_1(Q^2)$ and $x_1(Q^2)$, which are defined as

$$g_1(Q^2) = F_1^A(Q^2) + D_1^A(Q^2), \quad (17)$$

$$x_1(Q^2) = \frac{F_1^A(Q^2)}{F_1^A(Q^2) + D_1^A(Q^2)}; \quad (18)$$

where $F_1^A(Q^2)$ and $D_1^A(Q^2)$ are the antisymmetric and symmetric couplings of the two octets, determined from the semileptonic decays of hyperons at very low $Q^2 \approx 0$. It may be pointed out that there is no information available in the literature, for the Q^2 dependence of these parameters. Therefore, phenomenologically same Q^2 dependence for F_1^A and D_1^A , that is the dipole form is assumed, such that the parameter $x_1(Q^2)$ becomes a constant, *i.e.*, $x_1(Q^2) \approx x_1(0) = 0.364$.

The explicit expressions of $g_1^{NY}(Q^2)$ for $p \rightarrow \Lambda$, $p \rightarrow \Sigma^0$ and $n \rightarrow \Sigma^-$ are given as

$$g_1^{p\Lambda}(Q^2) = -\frac{1}{\sqrt{6}}(1 + 2x_1)g_1(Q^2), \quad (19)$$

$$g_1^{n\Sigma^-}(Q^2) = (1 - 2x_1)g_1(Q^2), \quad (20)$$

$$g_1^{p\Sigma^0}(Q^2) = \frac{1}{\sqrt{2}}(1 - 2x_1)g_1(Q^2), \quad (21)$$

where

$$g_1(Q^2) = \frac{g_A(0)}{\left(1 + \frac{Q^2}{M_A^2}\right)^2}, \quad (22)$$

with $g_A(0) = 1.267$ [71] and $M_A = 1.026$ GeV [72].

(iii) **Pseudoscalar form factor:**

The contribution of $g_3^{NY}(Q^2)$ in ν_τ ($\bar{\nu}_\tau$) – N scattering is significant due to the high value of m_τ . In literature, there exists two parameterizations, given by Marshak *et al.* [60] and by Nambu [73], for the pseudoscalar form factor in the $\Delta S = 1$ channel. In order to study the effect of the pseudoscalar form factor on the cross section and polarization observables, we have used both the parameterizations. The expression of the pseudoscalar form factor parameterized by Nambu [73] is given as:

$$g_3^{NY}(Q^2) = \frac{(M + M_Y)^2}{2(m_K^2 + Q^2)} g_1^{NY}(Q^2), \quad (23)$$

where m_K is the kaon mass.

In the parameterization of Marshak *et al.* [60], the expression for the pseudoscalar form factor is given as:

$$g_3^{NY}(Q^2) = \frac{(M + M_Y)^2}{2Q^2} \frac{g_1^{NY}(Q^2)(m_K^2 + Q^2) - m_K^2 g_1^{NY}(0)}{m_K^2 + Q^2}. \quad (24)$$

4. Form factors with SU(3) symmetry breaking effects

In the literature, SU(3) symmetry breaking effects have been studied by various groups [74–82] especially in the case of semileptonic decays of hyperons. In this work, we have studied the effect of SU(3) symmetry breaking parameterized in the two models by Faessler *et al.* [58] and Schlumpf [57]:

(A) **Faessler et al.** [58]:

The main features of the model may be summarized as:

- i) At the leading order, there is no symmetry breaking effect for the vector form factor $f_1^{NY}(Q^2)$ because of the Ademollo-Gatto theorem [83].
- ii) In the presence of SU(3) symmetry breaking, the value of $f_2^{NY}(Q^2)$ is modified from its SU(3) symmetric value $f_2^{NY}(Q^2)$ to $\mathcal{F}_2^{NY}(Q^2)$, as

$$f_2^{p\Lambda}(Q^2) \longrightarrow \mathcal{F}_2^{p\Lambda}(Q^2) = f_2^{p\Lambda}(Q^2) - \frac{1}{3\sqrt{6}} [H_1^V(Q^2) - 2H_2^V(Q^2) - 3H_3^V(Q^2) - 6H_4^V(Q^2)], \quad (25)$$

$$f_2^{n\Sigma^-}(Q^2) \longrightarrow \mathcal{F}_2^{n\Sigma^-}(Q^2) = f_2^{n\Sigma^-}(Q^2) - \frac{1}{3} [H_1^V(Q^2) + H_3^V(Q^2)], \quad (26)$$

$$f_2^{p\Sigma^0}(Q^2) \longrightarrow \mathcal{F}_2^{p\Sigma^0}(Q^2) = f_2^{p\Sigma^0}(Q^2) - \frac{1}{3\sqrt{2}} [H_1^V(Q^2) + H_3^V(Q^2)], \quad (27)$$

where $f_2^{NY}(Q^2)$ for the different $N - Y$ transitions are given in Eqs.(14)–(16) and $H_i^V(Q^2); i = 1 - 4$ are the SU(3) symmetry breaking terms. Since the symmetry breaking effects, in this model, are studied for the semileptonic decays of hyperons at very low Q^2 , *i.e.*, $Q^2 \simeq 0$, therefore, no information about the Q^2 dependence of $H_i^V(Q^2)$ is available in the literature. For simplicity, a dipole parameterization is assumed

$$H_i^V(Q^2) = \frac{H_i^V(0)}{\left(1 + \frac{Q^2}{M_V^2}\right)^2}, \quad i = 1 - 4 \quad (28)$$

where $M_V = 0.84$ GeV is the vector dipole mass, and the values of the couplings $H_i^V(0)$ are given in Ref. [58], and are here quoted as:

$$H_1^V(0) = -0.246, \quad H_2^V(0) = 0.096, \quad H_3^V(0) = 0.021, \quad H_4^V(0) = 0.030$$

Similarly, the axial vector form factor $g_1^{NY}(Q^2)$, in the presence of SU(3) symmetry breaking, is modified to $\mathcal{G}_1^{NY}(Q^2)$ as

$$g_1^{p\Lambda}(Q^2) \longrightarrow \mathcal{G}_1^{p\Lambda}(Q^2) = g_1^{p\Lambda}(Q^2) - \frac{1}{3\sqrt{6}} [H_1^A(Q^2) - 2H_2^A(Q^2) - 3H_3^A(Q^2) - 6H_4^A(Q^2)], \quad (29)$$

$$g_1^{n\Sigma^-}(Q^2) \longrightarrow \mathcal{G}_1^{n\Sigma^-}(Q^2) = g_1^{n\Sigma^-}(Q^2) - \frac{1}{3} [H_1^A(Q^2) + H_3^A(Q^2)], \quad (30)$$

$$g_1^{p\Sigma^0}(Q^2) \longrightarrow \mathcal{G}_1^{p\Sigma^0}(Q^2) = g_1^{p\Sigma^0}(Q^2) + \frac{1}{3\sqrt{2}} [H_1^A(Q^2) + H_3^A(Q^2)], \quad (31)$$

with $g_1^{NY}(Q^2)$ defined in Eqs.(19)–(21) and a dipole parameterization is assumed for $H_i^A(Q^2)$ as

$$H_i^A(Q^2) = \frac{H_i^A(0)}{\left(1 + \frac{Q^2}{M_A^2}\right)^2}; \quad i = 1 - 4 \quad (32)$$

where the couplings $H_i^A(0)$ are [58]

$$H_1^A(0) = -0.050, \quad H_2^A(0) = 0.011, \quad H_3^A(0) = -0.006, \quad H_4^A(0) = 0.037.$$

- iii) Since the pseudoscalar form factor is parameterized in terms of the axial vector form factor (Eqs. (23) and (24)), therefore, it receives SU(3) symmetry breaking effect *via.*, $g_1^{NY}(Q^2)$.

(B) **Schlumpf** [57]:

Schlumpf [57] has studied SU(3) symmetry breaking in the hadronic current containing vector (f_1) and axial vector (g_1) form factors using relativistic quark model, and this symmetry breaking in the model originates from the mass difference between m_s and $m_{u/d}$ quarks. The modified f_1 and g_1 form factors are given by

$$\begin{aligned} f_1(Q^2) &\rightarrow f_1'(Q^2) = \alpha f_1(Q^2) \\ g_1(Q^2) &\rightarrow g_1'(Q^2) = \beta g_1(Q^2), \text{ where} \end{aligned} \quad (33)$$

$\alpha=0.976, 0.975$ and 0.975 ; $\beta=1.072, 1.051$ and 1.056 , respectively for $p \rightarrow \Lambda$, $p \rightarrow \Sigma^0$ and $n \rightarrow \Sigma^-$ transitions. Since the induced pseudoscalar form factor g_3 is related to the axial vector form factor g_1 , therefore, this modification is also applicable to the terms containing g_3 through Eqs. (23) and (24).

III. CROSS SECTION AND POLARIZATION OBSERVABLES OF THE FINAL LEPTON

A. Cross section

The general expression of the differential cross section for the processes given in Eq. (1), in the laboratory frame, is given by

$$d\sigma = \frac{1}{(2\pi)^2} \frac{1}{4ME_{\bar{\nu}_\tau}} \delta^4(k+p-k'-p') \frac{d^3k'}{2E_{k'}} \frac{d^3p'}{2E_{p'}} \overline{\sum} \sum |\mathcal{M}|^2. \quad (34)$$

Using Eqs. (2)–(4), the transition matrix element squared is obtained as:

$$\overline{\sum} \sum |\mathcal{M}|^2 = \frac{G_F^2 \sin^2 \theta_c}{2} \mathcal{J}^{\mu\nu} \mathcal{L}_{\mu\nu}, \quad (35)$$

where the hadronic ($\mathcal{J}_{\mu\nu}$) and the leptonic ($\mathcal{L}_{\mu\nu}$) tensors are obtained using Eqs. (3) and (4) as

$$\mathcal{J}_{\mu\nu} = \overline{\sum} \sum J_\mu J_\nu^\dagger, \quad \mathcal{L}^{\mu\nu} = \overline{\sum} \sum l_\mu l_\nu^\dagger. \quad (36)$$

Following the above definitions, the differential scattering cross section $d\sigma/dQ^2$ for the processes given in Eq. (1) is written as

$$\frac{d\sigma}{dQ^2} = \frac{G_F^2 \sin^2 \theta_c}{8\pi M^2 E_{\bar{\nu}_\tau}^2} N(Q^2), \quad (37)$$

where $N(Q^2) = \mathcal{J}^{\mu\nu} \mathcal{L}_{\mu\nu}$ is obtained from the expression given in Appendix-A of Ref. [26] with the substitution of $M' = M_Y$ and $m_\mu = m_\tau$.

B. Polarization of the final lepton

Using the covariant density matrix formalism, the polarization 4-vector (ζ^τ) of the τ lepton produced in the final state in reactions given in Eq. (1) is written as [84]

$$\zeta^\tau = \frac{\text{Tr}[\gamma^\tau \gamma_5 \rho_f(k')]}{\text{Tr}[\rho_f(k')]}, \quad (38)$$

and the spin density matrix for the final lepton $\rho_f(k')$ is given by

$$\rho_f(k') = \mathcal{J}^{\alpha\beta} \text{Tr}[\Lambda(k') \gamma_\alpha (1 \pm \gamma_5) \Lambda(k) \tilde{\gamma}_\beta (1 \pm \tilde{\gamma}_5) \Lambda(k')], \quad (39)$$

with $\tilde{\gamma}_\alpha = \gamma^0 \gamma_\alpha^\dagger \gamma^0$ and $\tilde{\gamma}_5 = \gamma^0 \gamma_5^\dagger \gamma^0$.

Using the following relations:

$$\Lambda(k') \gamma^\tau \gamma_5 \Lambda(k') = 2m_\tau \left(g^{\tau\sigma} - \frac{k'^\tau k'^\sigma}{m_\tau^2} \right) \Lambda(k') \gamma_\sigma \gamma_5 \quad (40)$$

and

$$\Lambda(k') \Lambda(k') = 2m_\tau \Lambda(k'), \quad (41)$$

ζ^τ defined in Eq. (38) may also be rewritten as

$$\zeta^\tau = \left(g^{\tau\sigma} - \frac{k'^\tau k'^\sigma}{m_\tau^2} \right) \frac{\mathcal{J}^{\alpha\beta} \text{Tr}[\gamma_\sigma \gamma_5 \Lambda(k') \gamma_\alpha (1 + \gamma_5) \Lambda(k) \tilde{\gamma}_\beta (1 + \tilde{\gamma}_5)]}{\mathcal{J}^{\alpha\beta} \text{Tr}[\Lambda(k') \gamma_\alpha (1 + \gamma_5) \Lambda(k) \tilde{\gamma}_\beta (1 + \tilde{\gamma}_5)]}, \quad (42)$$

where m_τ is the mass of the τ lepton. In Eq. (42), the denominator is directly related to the differential cross section given in Eq. (37).

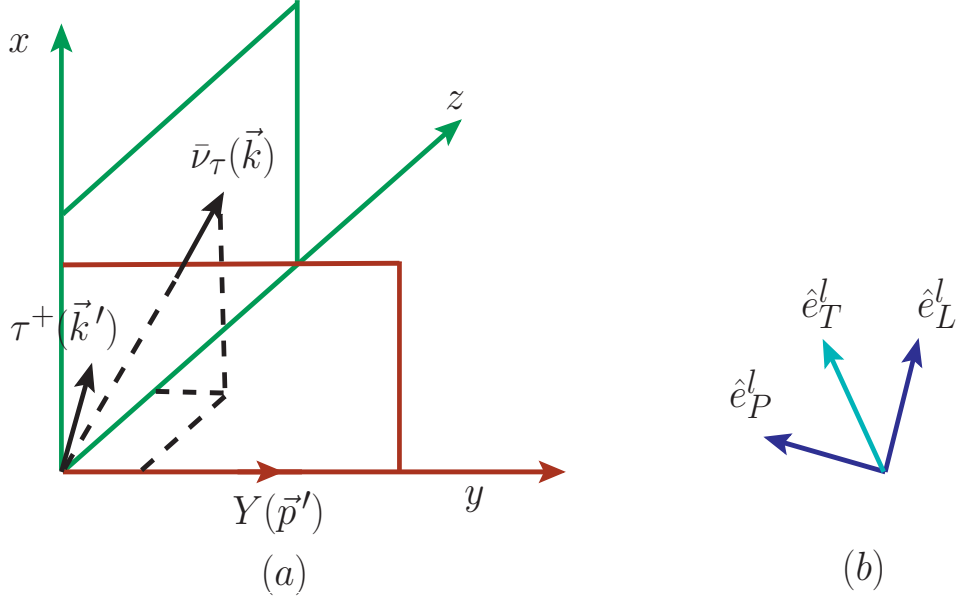


FIG. 2: (a) Momentum and polarization directions of the final lepton produced in the reaction $\bar{\nu}_\tau(k) + N(p) \rightarrow \tau^+(k') + Y(p')$. (b) \hat{e}_L^l , \hat{e}_P^l and \hat{e}_T^l represent the orthogonal unit vectors corresponding to the longitudinal, perpendicular and transverse directions with respect to the momentum of the final lepton.

With $\mathcal{J}^{\alpha\beta}$ and $\mathcal{L}_{\alpha\beta}$ given in Eq. (36), an expression for ζ^τ is obtained. In the laboratory frame where the initial nucleon is at rest, the polarization vector $\vec{\zeta}$, assuming T invariance, is calculated to be a function of 3-momenta of incoming antineutrino (\vec{k}) and outgoing lepton (\vec{k}'), and is given as

$$\vec{\zeta} = [A^l(Q^2)\vec{k} + B^l(Q^2)\vec{k}'], \quad (43)$$

where the expressions of $A^l(Q^2)$ and $B^l(Q^2)$ are obtained from the expression given in Appendix-B of Ref. [26] with the substitution $M' = M_Y$ and $m_\mu = m_\tau$.

One may expand the polarization vector $\vec{\zeta}$ along the orthogonal directions, \hat{e}_L^l , \hat{e}_P^l and \hat{e}_T^l in the reaction plane corresponding to the longitudinal, perpendicular and transverse directions of the final lepton (l), as depicted in Fig. 2 and defined as

$$\hat{e}_L^l = \frac{\vec{k}'}{|\vec{k}'|}, \quad \hat{e}_P^l = \hat{e}_L^l \times \hat{e}_T^l, \quad \text{where} \quad \hat{e}_T^l = \frac{\vec{k} \times \vec{k}'}{|\vec{k} \times \vec{k}'|}. \quad (44)$$

We then write $\vec{\zeta}$ as:

$$\vec{\zeta} = \zeta_L \hat{e}_L^l + \zeta_P \hat{e}_P^l + \zeta_T \hat{e}_T^l, \quad (45)$$

such that the longitudinal and perpendicular components of the $\vec{\zeta}$ in the laboratory frame are given by

$$\zeta_L(Q^2) = \vec{\zeta} \cdot \hat{e}_L^l, \quad \zeta_P(Q^2) = \vec{\zeta} \cdot \hat{e}_P^l. \quad (46)$$

From Eq. (46), the longitudinal $P_L(Q^2)$ and perpendicular $P_P(Q^2)$ components of the polarization vector defined in the rest frame of the outgoing lepton are given by

$$P_L(Q^2) = \frac{m_\tau}{E_{k'}} \zeta_L(Q^2), \quad P_P(Q^2) = \zeta_P(Q^2), \quad (47)$$

where $\frac{m_\tau}{E_{k'}}$ is the Lorentz boost factor along \vec{k}' . Using Eqs. (43), (44) and (46) in Eq. (47), the longitudinal $P_L(Q^2)$

and perpendicular $P_P(Q^2)$ components are calculated to be

$$P_L(Q^2) = \frac{m_\tau}{E_{k'}} \frac{A^l(Q^2) \vec{k} \cdot \vec{k}' + B^l(Q^2) |\vec{k}'|^2}{N(Q^2) |\vec{k}'|}, \quad (48)$$

$$P_P(Q^2) = \frac{A^l(Q^2) [|\vec{k}|^2 |\vec{k}'|^2 - (\vec{k} \cdot \vec{k}')^2]}{N(Q^2) |\vec{k}'| |\vec{k} \times \vec{k}'|}, \quad (49)$$

where $N(Q^2) = \mathcal{J}^{\mu\nu} \mathcal{L}_{\mu\nu}$ is obtained from the expression given in Appendix-A of Ref. [26].

IV. RESULTS AND DISCUSSION

In this section, we present and discuss the results of the differential (Section IV A) and total (Section IV B) scattering cross sections as well as the polarization observables of the final τ lepton produced in the $|\Delta S| = 1$ quasielastic scattering of $\bar{\nu}_\tau$ from nucleons. We also present a comparison of the total cross section for the production of e , μ and τ leptons in the quasielastic scattering of $\bar{\nu}_e$, $\bar{\nu}_\mu$ and $\bar{\nu}_\tau$ to demonstrate the implications of LFU in these processes (Section IV C).

A. Differential scattering cross section and polarization observables

We have used Eqs. (37), (48) and (49), respectively, to numerically evaluate the differential scattering cross section $d\sigma/dQ^2$, the longitudinal ($P_L(Q^2)$) and the perpendicular ($P_P(Q^2)$) components of polarization of τ lepton. The Dirac and Pauli form factors $f_{1,2}^N(Q^2)$; ($N = p, n$) are expressed in terms of the electric and magnetic Sachs' form factors, for which the various parameterizations [63–68] available in the literature, have been used. For $g_1(Q^2)$ a dipole parameterization has been used (Eq. (22)), with the world average value of the axial dipole mass $M_A = 1.026$ GeV. For the pseudoscalar form factor $g_3(Q^2)$, the parameterizations given by Nambu [73] and Marshak *et al.* [60] have been used. The numerical results of the differential scattering cross section and polarization observables obtained assuming SU(3) symmetry and the results with SU(3) symmetry breaking effects, using the prescriptions of: (i) Faessler *et al.* [58], and (ii) Schlumpf [57], are presented separately for the Λ and Σ^- productions from the nucleons. The results for the Σ^0 production can be expressed in terms of the Σ^- production in the SU(3) symmetric limit (Eqs. (10 and 11)) and are not presented separately.

1. Λ production

In Fig. 3, we present the results for the Q^2 distribution *i.e.* $\frac{d\sigma}{dQ^2}$, $P_L(Q^2)$ and $P_P(Q^2)$ vs Q^2 for $\bar{\nu}_\tau + p \rightarrow \tau^+ + \Lambda$ process at the three different values of energy viz. $E_{\bar{\nu}_\tau} = 4$ GeV, 5 GeV and 10 GeV, assuming SU(3) symmetry with $M_A = 1.026$ GeV and using the different parameterizations of the nucleon vector form factors *viz.*, BBBA05 [63], BBA03 [65], Alberico [66], Bosted [64], Galster [68] and Kelly [67]. We see that at low $\bar{\nu}_\tau$ energies, for example at $E_{\bar{\nu}_\tau} = 4$ GeV, there is considerable dependence of the different parameterizations of the vector form factors on $\frac{d\sigma}{dQ^2}$, $P_L(Q^2)$ and $P_P(Q^2)$ distributions. However, with the increase in $\bar{\nu}_\tau$ energy, this difference decreases and becomes almost negligible at higher energies, like at $E_{\bar{\nu}_\tau} = 10$ GeV, especially for $\frac{d\sigma}{dQ^2}$ and $P_L(Q^2)$ distributions.

To study the effect of the variation in M_A (in the range 0.9–1.3 GeV) on the differential cross section and polarization observables, we present, in Fig. 4, the results for $\frac{d\sigma}{dQ^2}$, $P_L(Q^2)$ and $P_P(Q^2)$ distributions at $E_{\bar{\nu}_\tau} = 4$ GeV, 5 GeV and 10 GeV. We find that at low $\bar{\nu}_\tau$ energies, there is a significant dependence of these distributions on the choice of M_A . With the increase in $\bar{\nu}_\tau$ energy, this dependence on the variation in M_A decreases, especially for $\frac{d\sigma}{dQ^2}$ and to some extent for $P_L(Q^2)$ but not for $P_P(Q^2)$ distribution. Moreover, it is important to point out that in the case of $\bar{\nu}_\tau + p \rightarrow \tau^+ + \Lambda$ reaction, with the increase in M_A , $\frac{d\sigma}{dQ^2}$ decreases (0.9 GeV to 1.1 GeV), but with the further increase in M_A (1.1 GeV to 1.3 GeV), $\frac{d\sigma}{dQ^2}$ increases, which is not generally the case in $\nu_l + n \rightarrow l^- + p$; ($l = e, \mu, \tau$) scattering. Moreover, in the case of $\bar{\nu}_l + p \rightarrow l^+ + n$, we have observed that with the increase in M_A , $\frac{d\sigma}{dQ^2}$ decreases (from 0.9 GeV to 1.1 GeV) and with further increase in $M_A = 1.2$ GeV, $\frac{d\sigma}{dQ^2}$ increases [17]. In the present work, for Λ production we observe similar trend as in the case of $\bar{\nu}_\tau$ induced CCQE reaction [17]. In the $\bar{\nu}_\tau$ induced reactions because of the production of massive τ lepton in the final state, the pseudoscalar form factor becomes significant. The variation in

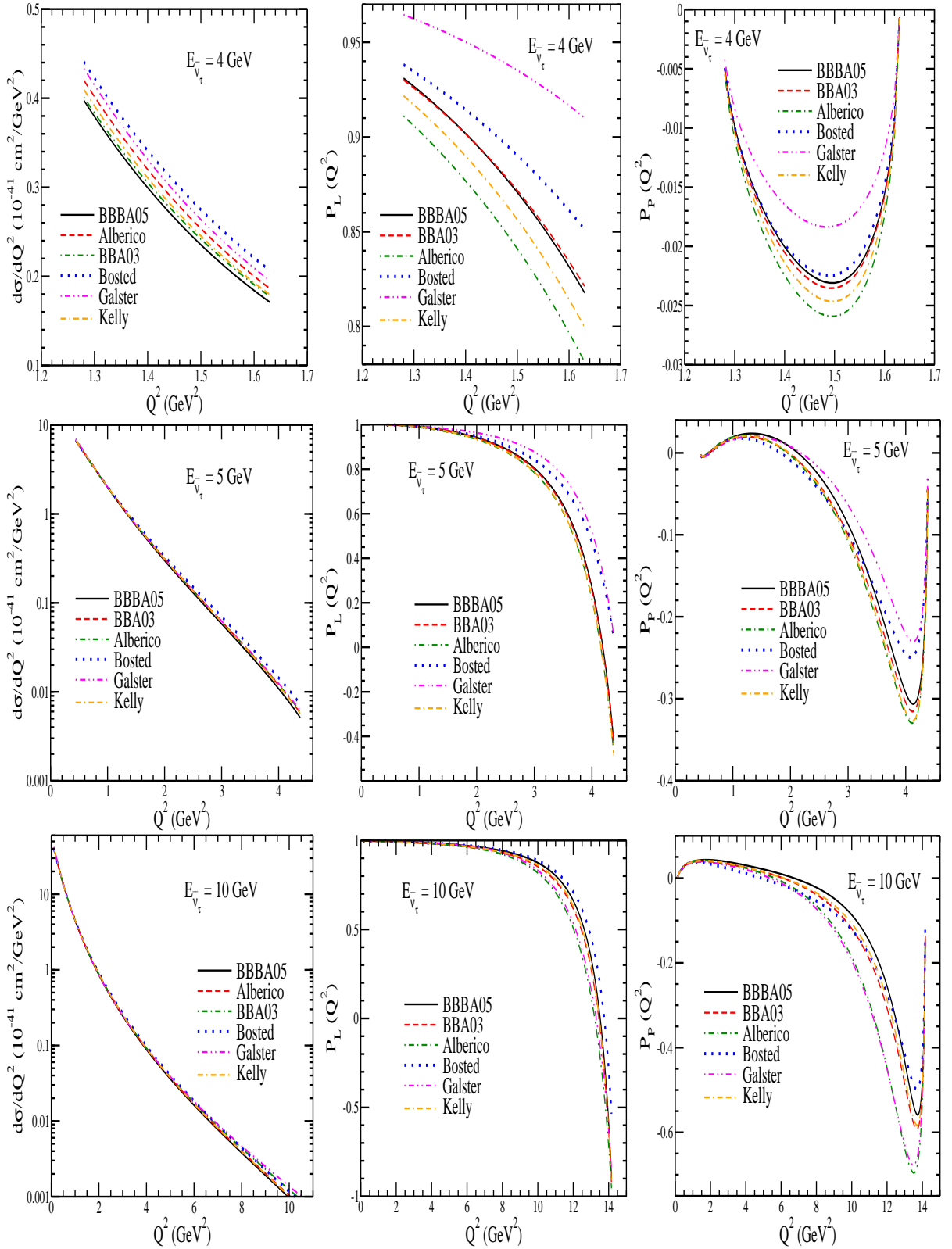


FIG. 3: $\frac{d\sigma}{dQ^2}$ (left panel), $P_L(Q^2)$ (middle panel) and $P_P(Q^2)$ (right panel) versus Q^2 for the process $\bar{\nu}_\tau + p \rightarrow \tau^+ + \Lambda$ at $E_{\bar{\nu}_\tau} = 4$ GeV (upper panel), 5 GeV (middle panel) and 10 GeV (lower panel). The calculations have been performed using the SU(3) symmetry with the axial dipole mass $M_A = 1.026$ GeV and for the different parameterizations of the nucleon vector form factors *viz.*, BBBA05 [63] (solid line), BBA03 [65] (dashed line), Alberico *et al.* [66] (dashed-dotted line), Bosted [64] (dotted line), Galster *et al.* [68] (double-dotted-dashed line) and Kelly [67] (double-dashed-dotted line).

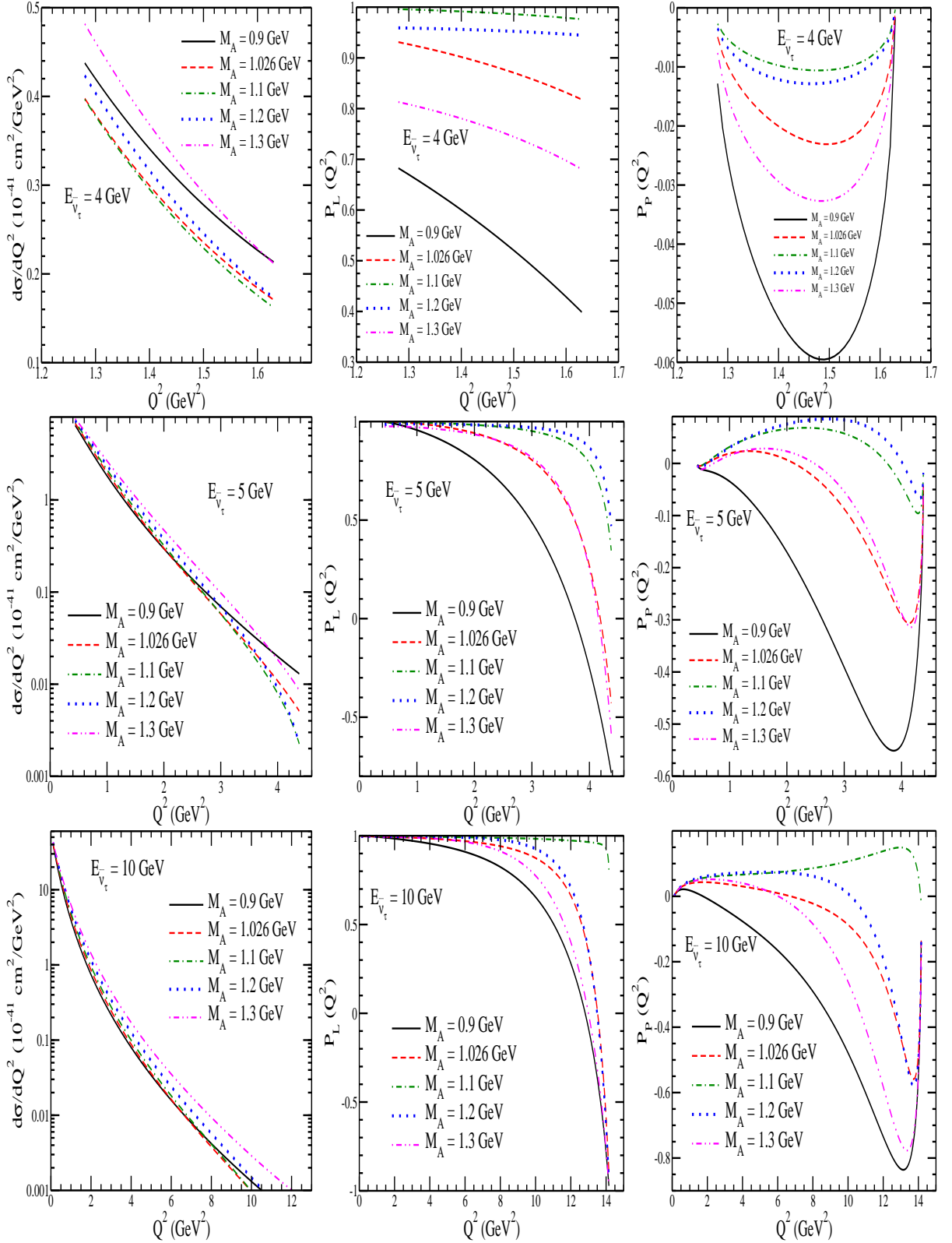


FIG. 4: $\frac{d\sigma}{dQ^2}$ (left panel), $P_L(Q^2)$ (middle panel) and $P_P(Q^2)$ (right panel) versus Q^2 for the process $\bar{\nu}_\tau + p \rightarrow \tau^+ + \Lambda$ at $E_{\bar{\nu}_\tau} = 4$ GeV (upper panel), 5 GeV (middle panel) and 10 GeV (lower panel). The calculations have been performed using the SU(3) symmetry with the electric and magnetic Sachs form factors parameterized by Bradford *et al.* [63] and for the axial form factor, the different values of M_A have been used *viz.* $M_A = 0.9$ GeV (solid line), 1.026 GeV (dashed line), 1.1 GeV (dashed-dotted line), 1.2 GeV (dotted line) and 1.3 GeV (double-dotted-dashed line).

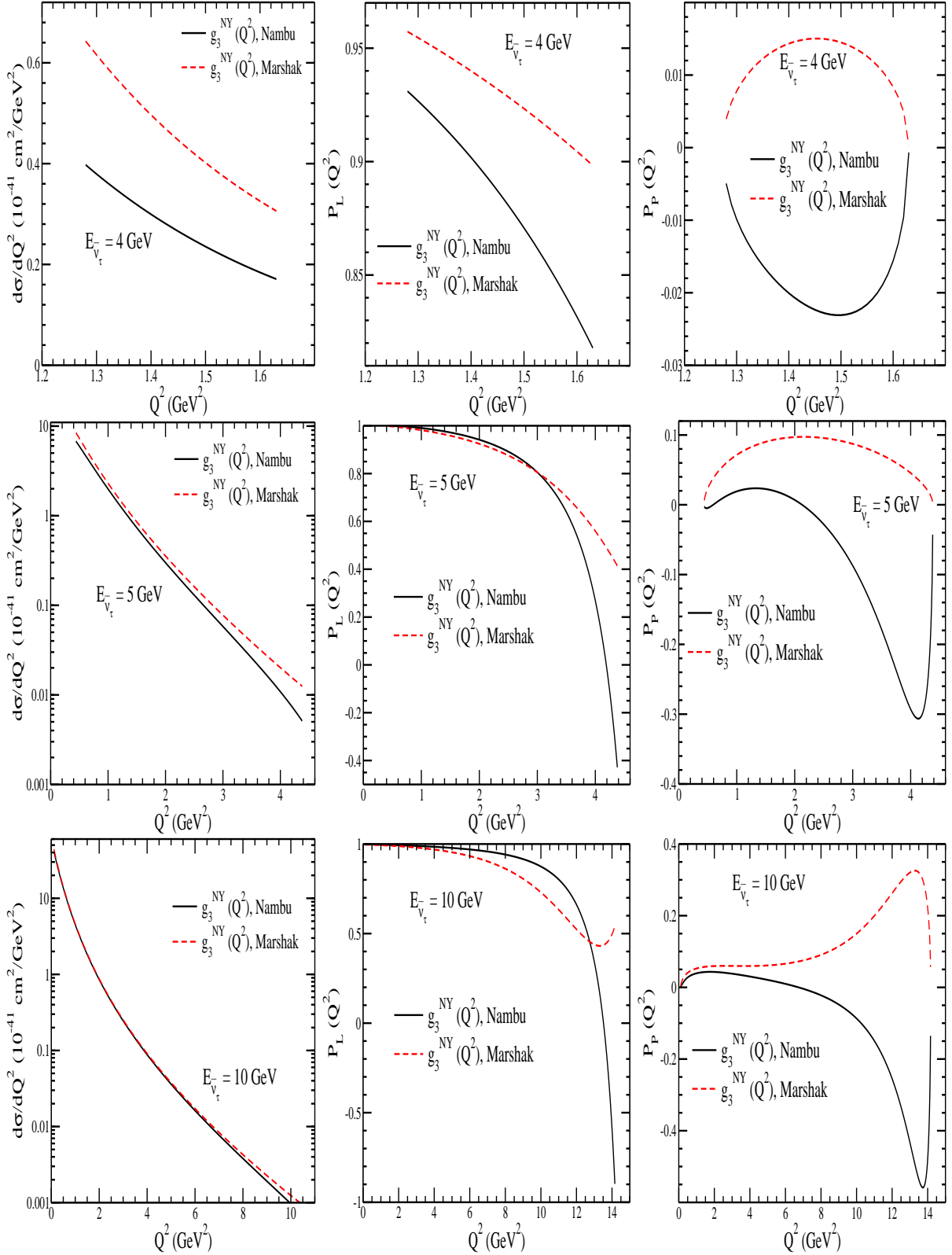


FIG. 5: $\frac{d\sigma}{dQ^2}$ (left panel), $P_L(Q^2)$ (middle panel) and $P_P(Q^2)$ (right panel) versus Q^2 for the process $\bar{\nu}_\tau + p \rightarrow \tau^+ + \Lambda$ at $E_{\bar{\nu}_\tau} = 4$ GeV (upper panel), 5 GeV (middle panel) and 10 GeV (lower panel). The calculations have been performed using the SU(3) symmetry with the electric and magnetic Sachs form factors parameterized by Bradford *et al.* [63], $M_A = 1.026$ GeV, and for the different parameterizations of the pseudoscalar scalar form factor, *viz.* the parameterizations given by Nambu [73] (solid line) and by Marshak *et al.* [60] (dashed line).

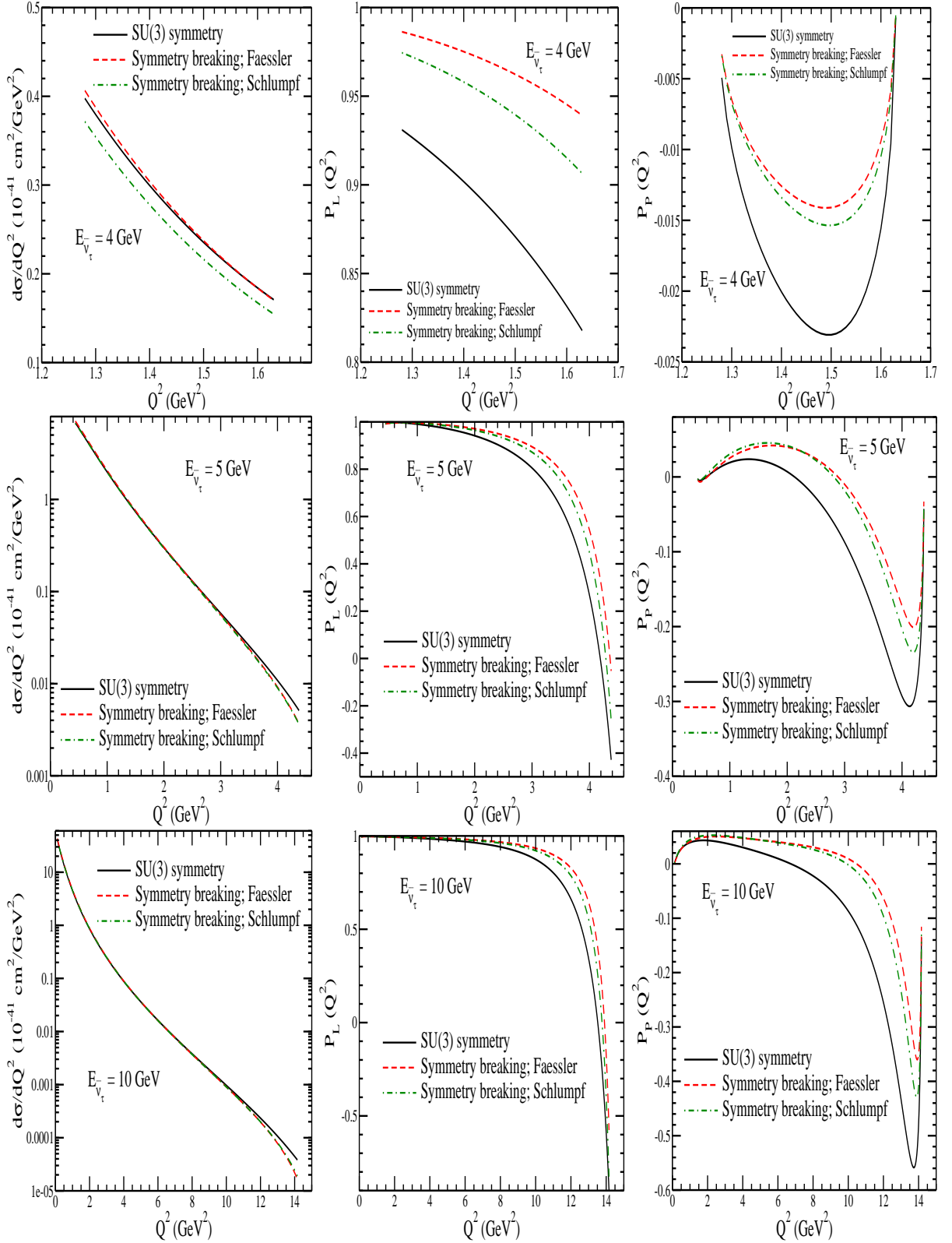


FIG. 6: $\frac{d\sigma}{dQ^2}$ (left panel), $P_L(Q^2)$ (middle panel) and $P_P(Q^2)$ (right panel) versus Q^2 for the process $\bar{\nu}_\tau + p \rightarrow \tau^+ + \Lambda$ at $E_{\bar{\nu}_\tau} = 4$ GeV (upper panel), 5 GeV (middle panel) and 10 GeV (lower panel). The calculations have been performed with $M_A = 1.026$ GeV and BBBA05 [63] for the vector form factors with SU(3) symmetry (solid line), SU(3) symmetry breaking effects parameterized by Faessler *et al.* [58] (dashed line) and the symmetry breaking effects parameterized by Schlumpf [57] (dashed-dotted line).

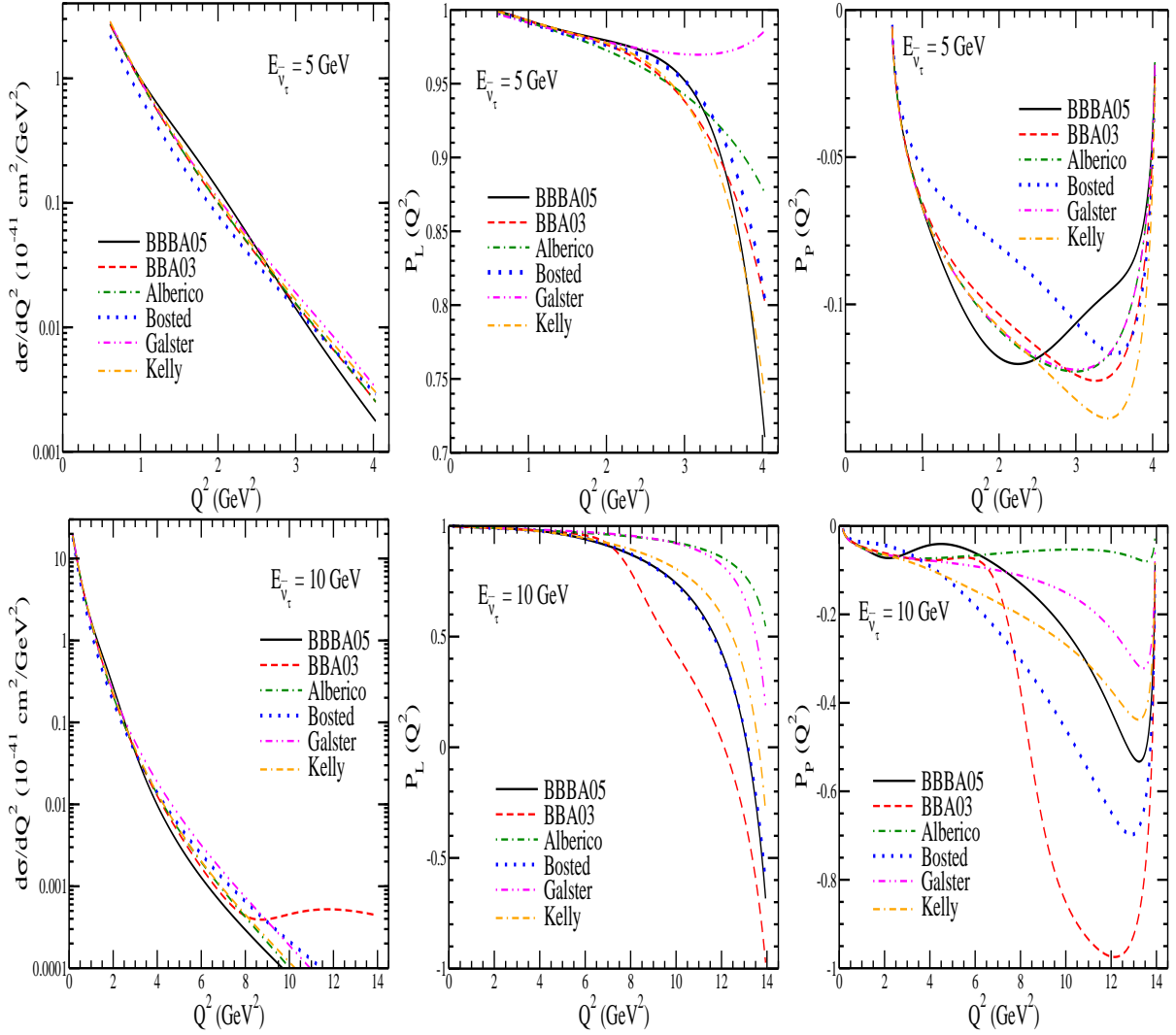


FIG. 7: $\frac{d\sigma}{dQ^2}$ (left panel), $P_L(Q^2)$ (middle panel) and $P_P(Q^2)$ (right panel) versus Q^2 for the process $\bar{\nu}_\tau + n \rightarrow \tau^+ + \Sigma^-$ at $E_{\bar{\nu}_\tau} = 5$ GeV (upper panel) and 10 GeV (lower panel). The calculations have been performed using the SU(3) symmetry with the axial dipole mass $M_A = 1.026$ GeV and for the different parameterizations of the nucleon vector form factors *viz.*, BBBA05 [63] (solid line), BBA03 [65] (dashed line), Alberico *et al.* [66] (dashed-dotted line), Bosted [64] (dotted line), Galster *et al.* [68] (double-dotted-dashed line) and Kelly [67] (double-dashed-dotted line).

$\frac{d\sigma}{dQ^2}$ observed in Fig. 4 arises due to interference of the pseudoscalar form factor with axial vector and vector form factors.

To see the dependence of $\frac{d\sigma}{dQ^2}$, $P_L(Q^2)$ and $P_P(Q^2)$ on the pseudoscalar form factor $g_3^{NY}(Q^2)$, we have used the two parameterizations of $g_3^{NY}(Q^2)$ given in Eqs. (23) by Nambu [73], and (24) by Marshak *et al.* [60], and show the numerical results in Fig. 5. It may be observed that at low $\bar{\nu}_\tau$ energies, there is a large dependence on the choice of $g_3^{NY}(Q^2)$. While with the increase in $E_{\bar{\nu}_\tau}$, this dependence on the choice of $g_3^{NY}(Q^2)$ becomes almost negligible for the $\frac{d\sigma}{dQ^2}$ distribution, whereas for $P_L(Q^2)$ and $P_P(Q^2)$ distributions, they are found to be quite significant, even for the higher values of $E_{\bar{\nu}_\tau}$, say $E_{\bar{\nu}_\tau} = 10$ GeV.

In Fig. 6, we present the results for $\frac{d\sigma}{dQ^2}$, $P_L(Q^2)$ and $P_P(Q^2)$ vs Q^2 at $E_{\bar{\nu}_\tau} = 4$ GeV, 5 GeV and 10 GeV, when the SU(3) symmetry breaking effects are taken into account following the prescription of Faessler *et al.* [58] and Schlumpf [57]. We observe that at low $\bar{\nu}_\tau$ energies, for example at $E_{\bar{\nu}_\tau} = 4$ GeV, there is some effect of SU(3) symmetry breaking on the $\frac{d\sigma}{dQ^2}$ distribution if the parameterization by Schlumpf [57] is used, while there is almost no effect if one uses the parameterization of Faessler *et al.* [58]. However, in the case of $P_L(Q^2)$ and $P_P(Q^2)$, there is some effect of SU(3) breaking using either the prescription of Faessler *et al.* [58] or Schlumpf [57]. Moreover, with the increase in $\bar{\nu}_\tau$ energy, the difference in $\frac{d\sigma}{dQ^2}$ due to the use of the two parameterizations of SU(3) symmetry breaking

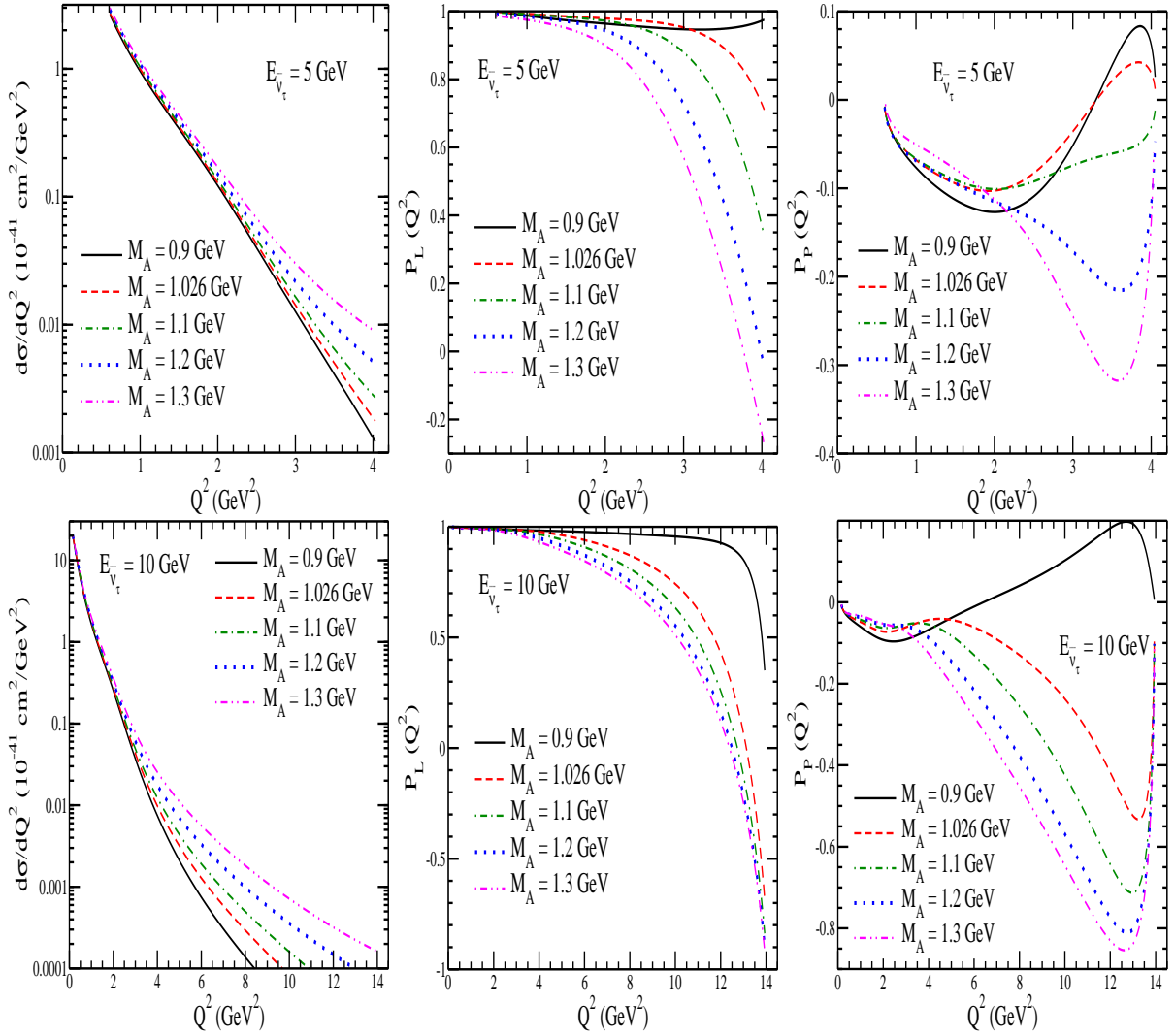


FIG. 8: $\frac{d\sigma}{dQ^2}$ (left panel), $P_L(Q^2)$ (middle panel) and $P_P(Q^2)$ (right panel) versus Q^2 for the process $\bar{\nu}_\tau + n \rightarrow \tau^+ + \Sigma^-$ at $E_{\bar{\nu}_\tau} = 5$ GeV (upper panel) and 10 GeV (lower panel). The calculations have been performed using the SU(3) symmetry with the electric and magnetic Sachs form factors parameterized by Bradford *et al.* [63] and for the axial form factor, the different values of M_A have been used *viz.* $M_A = 0.9$ GeV (solid line), 1.026 GeV (dashed line), 1.1 GeV (dashed-dotted line), 1.2 GeV (dotted line) and 1.3 GeV (double-dotted-dashed line).

becomes almost negligible at higher energies. In the case of polarization observables, the two parameterizations of SU(3) symmetry breaking give different results for all the values of Q^2 .

2. Σ^- production

In Fig. 7, we present the results for $\frac{d\sigma}{dQ^2}$, $P_L(Q^2)$ and $P_P(Q^2)$ vs Q^2 for the process $\bar{\nu}_\tau + n \rightarrow \tau^+ + \Sigma^-$ at the two different value of energies *viz.* $E_{\bar{\nu}_\tau} = 5$ GeV and 10 GeV, using the different parameterizations of the nucleon vector form factors *viz.*, BBBA05 [63], BBA03 [65], Alberico [66], Bosted [64], Galster [68] and Kelly [67]. We observe that at low $\bar{\nu}_\tau$ energies, for example at $E_{\bar{\nu}_\tau} = 5$ GeV, there is considerable dependence of the different parameterizations of the vector form factors on $\frac{d\sigma}{dQ^2}$, $P_L(Q^2)$ and $P_P(Q^2)$ distributions. However, unlike the case of Λ production (Fig. 4), with the increase in $\bar{\nu}_\tau$ energy, this difference further increases and becomes quite significant at higher energies, especially for the distributions of the polarization observables $P_L(Q^2)$ and $P_P(Q^2)$.

The effect of M_A variation on the differential cross section and polarization observables are presented in Fig. 8, at $E_{\bar{\nu}_\tau} = 5$ GeV and 10 GeV by varying M_A in the range 0.9–1.3 GeV. We find that at low $\bar{\nu}_\tau$ energies, there is large

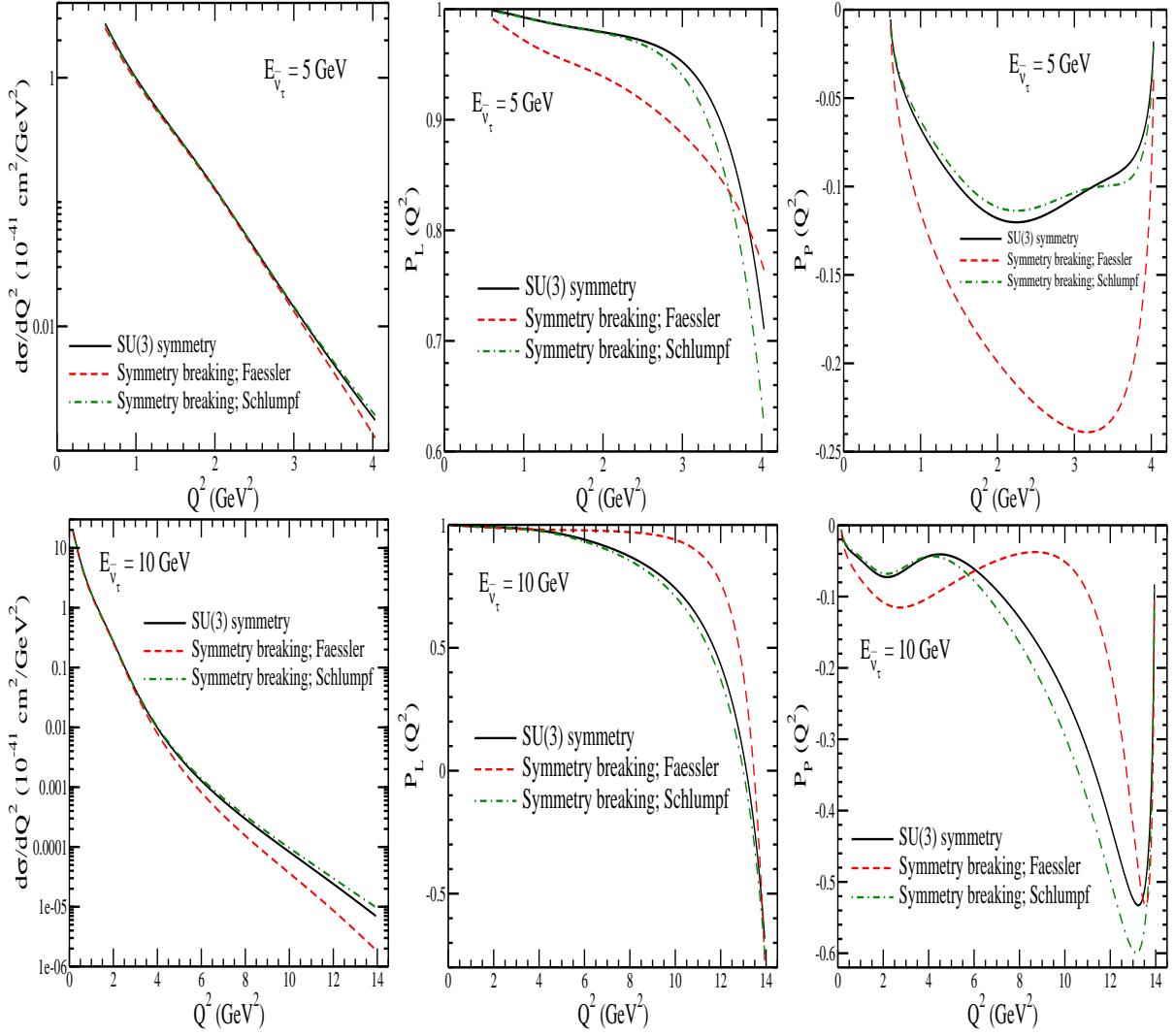


FIG. 9: $\frac{d\sigma}{dQ^2}$ (left panel), $P_L(Q^2)$ (middle panel) and $P_P(Q^2)$ (right panel) versus Q^2 for the process $\bar{\nu}_\tau + n \rightarrow \tau^+ + \Sigma^-$ at $E_{\bar{\nu}_\tau} = 5 \text{ GeV}$ (upper panel) and 10 GeV (lower panel). The calculations have been performed with $M_A = 1.026 \text{ GeV}$ assuming SU(3) symmetry (solid line), as well as with SU(3) symmetry breaking effects parameterized by Faessler *et al.* [58] (dashed line) and by Schlumpf [57] (dashed-dotted line).

dependence of these distributions on the choice of M_A , which increases with increase in antineutrino energy.

In Fig. 9, we show the effect of SU(3) symmetry breaking by taking into account the parameterizations given by Faessler *et al.* [58] and Schlumpf [57] on $\frac{d\sigma}{dQ^2}$, $P_L(Q^2)$ and $P_P(Q^2)$ vs Q^2 at $E_{\bar{\nu}_\tau} = 5 \text{ GeV}$ and 10 GeV . From the figure, it may be observed that in the case of $\frac{d\sigma}{dQ^2}$, at low energies, say $E_{\bar{\nu}_\tau} = 5 \text{ GeV}$, the effect of SU(3) symmetry breaking is quite small. While at higher energies, say $E_{\bar{\nu}_\tau} = 10 \text{ GeV}$, the effect of SU(3) breaking is seen in the model of Faessler *et al.* [58] but not in the model of Schlumpf [57]. Whereas the polarization observables (both $P_L(Q^2)$ and $P_P(Q^2)$) are quite sensitive to SU(3) symmetry breaking effect, and there is considerable change in the results obtained using the two different choices of parameterizing the SU(3) symmetry breaking effect.

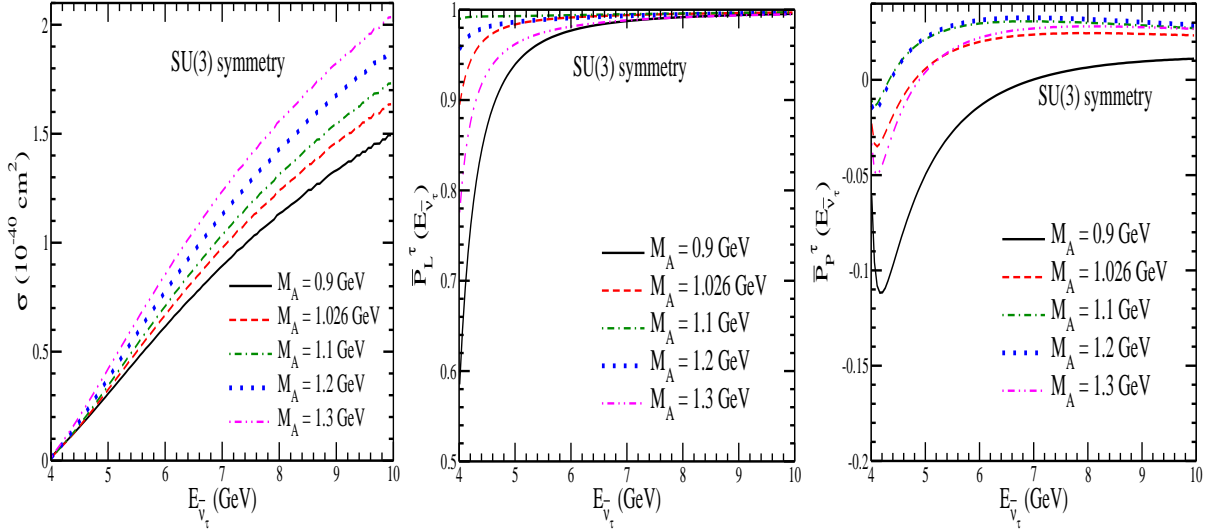


FIG. 10: σ (left panel), $\bar{P}_L(E_{\bar{\nu}_\tau})$ (middle panel), and $\bar{P}_P(E_{\bar{\nu}_\tau})$ (right panel) vs $E_{\bar{\nu}_\tau}$ for $\bar{\nu}_\tau + p \rightarrow \tau^+ + \Lambda$ process. The calculations have been performed using the SU(3) symmetry with electric and magnetic Sachs form factors parameterized by Bradford *et al.* [63] and for the axial form factor, the different values of M_A have been used *viz.* $M_A = 0.9$ GeV (solid line), 1.026 GeV (dashed line), 1.1 GeV (dashed-dotted line), 1.2 GeV (dotted line) and 1.3 GeV (double-dotted-dashed line).

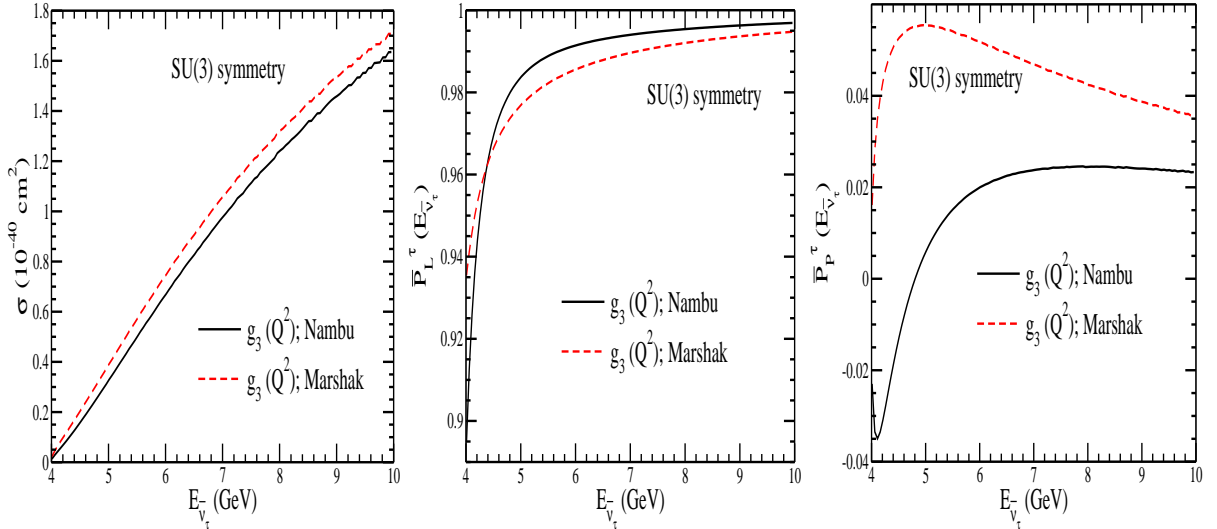


FIG. 11: σ (left panel), $\bar{P}_L(E_{\bar{\nu}_\tau})$ (middle panel), and $\bar{P}_P(E_{\bar{\nu}_\tau})$ (right panel) vs $E_{\bar{\nu}_\tau}$ for $\bar{\nu}_\tau + p \rightarrow \tau^+ + \Lambda$ process. The calculations have been performed using the SU(3) symmetry with electric and magnetic Sachs form factors parameterized by Bradford *et al.* [63] and for the axial form factor, $M_A = 1.026$ GeV is used, with the different parameterizations of the pseudoscalar form factor *viz.*, using the parameterizations given by Nambu [73] (solid line) and Marshak *et al.* [60] (dashed line).

B. Total scattering cross section and average polarizations

To study the dependence of the total scattering cross section $\sigma(E_{\bar{\nu}_\tau})$ and the average polarizations $\bar{P}_{L,P}(E_{\bar{\nu}_\tau})$ on $E_{\bar{\nu}_\tau}$, we have integrated $d\sigma/dQ^2$ and $P_{L,P}(Q^2)$ over Q^2 , and obtained the expressions for $\sigma(E_{\bar{\nu}_\tau})$ and $\bar{P}_{L,P}(E_{\bar{\nu}_\tau})$ *i.e.*:

$$\sigma(E_{\bar{\nu}_\tau}) = \int_{Q_{min}^2}^{Q_{max}^2} \frac{d\sigma}{dQ^2} dQ^2, \quad (50)$$

$$\bar{P}_{L,P}(E_{\bar{\nu}_\tau}) = \frac{\int_{Q_{min}^2}^{Q_{max}^2} P_{L,P}(Q^2) \frac{d\sigma}{dQ^2} dQ^2}{\int_{Q_{min}^2}^{Q_{max}^2} \frac{d\sigma}{dQ^2} dQ^2}. \quad (51)$$

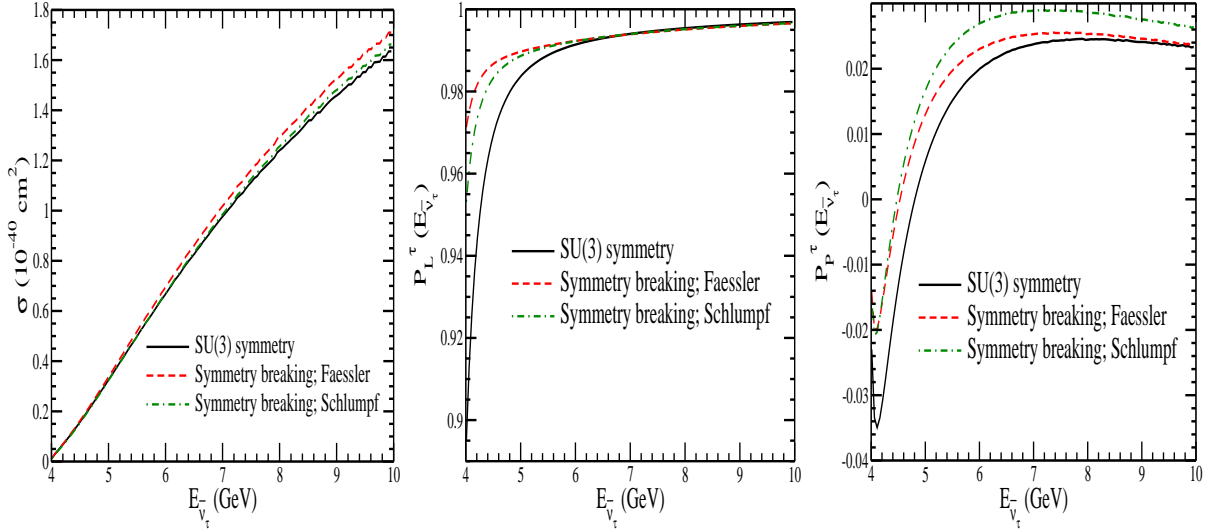


FIG. 12: σ (left panel), $\overline{P}_L(E_{\bar{\nu}_\tau})$ (middle panel), and $\overline{P}_P(E_{\bar{\nu}_\tau})$ (right panel) vs $E_{\bar{\nu}_\tau}$ for $\bar{\nu}_\tau + p \rightarrow \tau^+ + \Lambda$ process. The calculations have been performed using the SU(3) symmetry (solid line), the SU(3) symmetry breaking effects parameterized by Faessler *et al.* [58] (dashed line) and by Schlumpf [57] (dashed-dotted line), with electric and magnetic Sachs form factors parameterized by Bradford *et al.* [63] and for the axial form factor, $M_A = 1.026$ GeV is used.

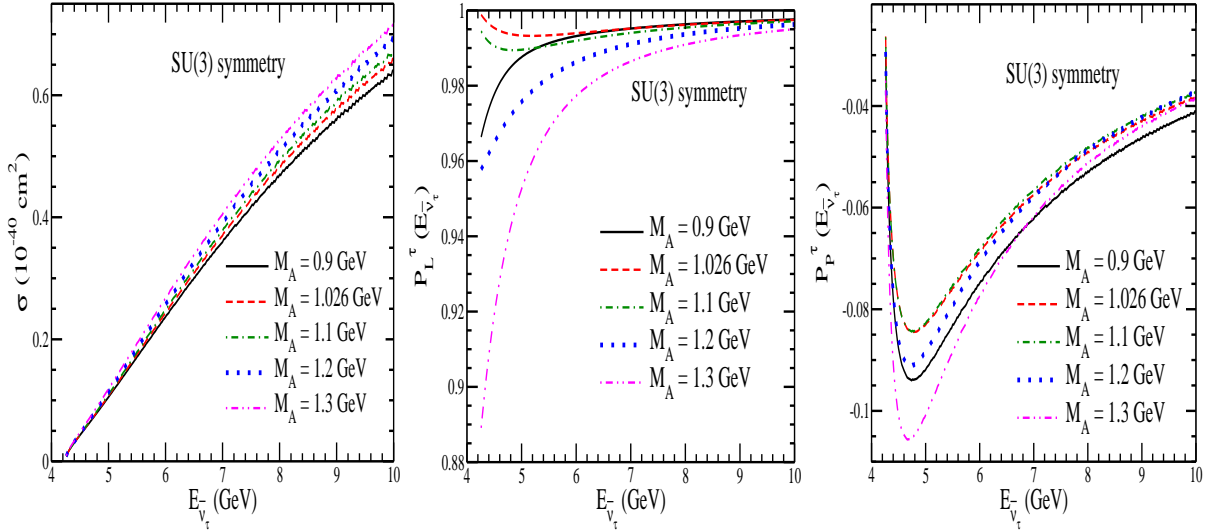


FIG. 13: σ (left panel), $\overline{P}_L(E_{\bar{\nu}_\tau})$ (middle panel), and $\overline{P}_P(E_{\bar{\nu}_\tau})$ (right panel) vs $E_{\bar{\nu}_\tau}$ for $\bar{\nu}_\tau + n \rightarrow \tau^+ + \Sigma^-$ process. The calculations have been performed using the SU(3) symmetry with the electric and magnetic Sachs form factors parameterized by Bradford *et al.* [63] and for the axial form factor, the different values of M_A have been used *viz.* $M_A = 0.9$ GeV (solid line), 1.026 GeV (dashed line), 1.1 GeV (dashed-dotted line), 1.2 GeV (dotted line) and 1.3 GeV (double-dotted-dashed line).

In this section, we present the results for the total cross section (Eq. (50)) and average polarizations (Eq. 51) of the tau lepton produced in $\bar{\nu}_\tau + N \rightarrow \tau^+ + Y$ reaction, separately for Λ and Σ^- productions, in Sections IV B 1 and IV B 2, respectively.

1. Λ production

In Fig. 10, the results are presented for σ as well as for $\overline{P}_L(E_{\bar{\nu}_\tau})$ and $\overline{P}_P(E_{\bar{\nu}_\tau})$ obtained using the different values of M_A *viz.* $M_A = 0.9, 1.026, 1.1, 1.2$ and 1.3 GeV for the process $\bar{\nu}_\tau + p \rightarrow \tau^+ + \Lambda$. As expected, σ increases with the increase in antineutrino energy as well as it increases in magnitude with higher values of M_A . For example, at $E_{\bar{\nu}_\tau} = 10$ GeV, σ increases by about 25%, when the value of M_A is increased from its world average value ($M_A =$

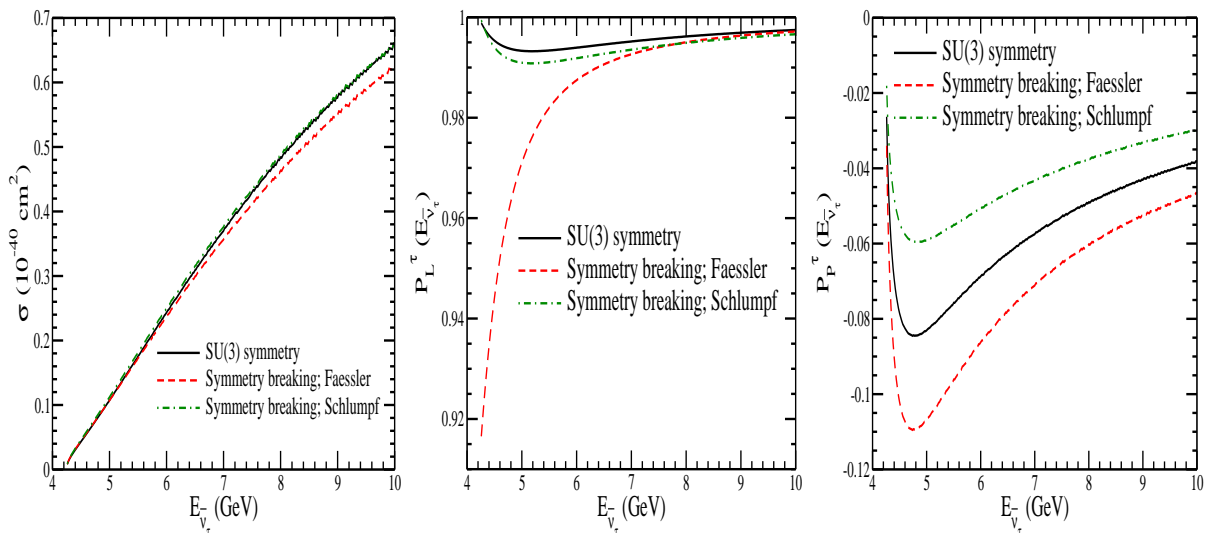


FIG. 14: σ (left panel), $\overline{P}_L(E_{\bar{\nu}_\tau})$ (middle panel), and $\overline{P}_P(E_{\bar{\nu}_\tau})$ (right panel) vs $E_{\bar{\nu}_\tau}$ for $\bar{\nu}_\tau + n \rightarrow \tau^+ + \Sigma^-$ process. The calculations have been performed using the SU(3) symmetry (solid line), the SU(3) symmetry breaking effects parameterized by Faessler *et al.* [58] (dashed line) and by Schlumpf [57] (dashed-dotted line), with electric and magnetic Sachs form factors parameterized by Bradford *et al.* [63] and for the axial form factor, $M_A = 1.026$ GeV is used.

1.026 GeV) by 30% and a decrease in the value of M_A by 10% from the world average value, decreases the cross section by $\sim 7\%$. At low antineutrino energies $E_{\bar{\nu}_\tau} = 4$ GeV, $\overline{P}_L(E_{\bar{\nu}_\tau})$ increases with the increase in M_A , which is almost 40% when M_A is varied from 0.9 to 1.3 GeV. However, with the increase in $E_{\bar{\nu}_\tau}$, this variation in $\overline{P}_L(E_{\bar{\nu}_\tau})$ decreases and becomes almost negligible at $E_{\bar{\nu}_\tau} = 10$ GeV. We observe some dependence of M_A on $\overline{P}_P(E_{\bar{\nu}_\tau})$ in the entire range of $E_{\bar{\nu}_\tau}$. Note that in the case of Λ production, σ , $\overline{P}_L(E_{\bar{\nu}_\tau})$ and $\overline{P}_P(E_{\bar{\nu}_\tau})$ are almost insensitive to the different parameterizations of the Sachs' form factors, and are not shown here explicitly.

In Fig. 11, we show the dependence of σ and $\overline{P}_{L,P}(E_{\bar{\nu}_\tau})$ on the pseudoscalar form factor, when the parameterizations by Marshak *et al.* [60] and Nambu [73] are used in the numerical calculations. It may be observed from the figure that σ as well as the average polarizations show some dependence on the pseudoscalar form factor.

In Fig. 12, we present the results for σ , $\overline{P}_L(E_{\bar{\nu}_\tau})$ and $\overline{P}_P(E_{\bar{\nu}_\tau})$ with SU(3) symmetry as well as when the SU(3) symmetry breaking effects are taken into account following the prescriptions of Faessler *et al.* [58] and Schlumpf [57]. We find that there is not much effect of SU(3) symmetry breaking on σ , while there is some effect on $\overline{P}_L(E_{\bar{\nu}_\tau})$ whereas in the case of $\overline{P}_P(E_{\bar{\nu}_\tau})$, the effect is found to be significant.

2. Σ^- production

The dependence of the total cross section and the average polarizations on M_A are shown in Fig. 13, where we present the results for σ and $\overline{P}_{L,P}(E_{\bar{\nu}_\tau})$ for the process $\bar{\nu}_\tau + n \rightarrow \tau^+ + \Sigma^-$ by varying M_A in the range, $M_A = 0.9$ to 1.3 GeV. The results are qualitatively similar to the results obtained in Fig. 10 for the $\bar{\nu}_\tau$ induced Λ production. σ increases with increase in the value of M_A and shows considerable variation at higher antineutrino energies. The average polarizations are quite sensitive to the variation in M_A , especially at low $E_{\bar{\nu}_\tau}$.

In Fig. 14, we show the results for σ , $\overline{P}_L(E_{\bar{\nu}_\tau})$ and $\overline{P}_P(E_{\bar{\nu}_\tau})$ with SU(3) symmetry as well as when the SU(3) symmetry breaking effects are taken into account. We find the effect of SU(3) symmetry breaking to be quite small on σ . In the case of $\overline{P}_L(E_{\bar{\nu}_\tau})$, the effect of SU(3) symmetry breaking is more when Faessler *et al.* [58] prescription is used. While in the case of $\overline{P}_P(E_{\bar{\nu}_\tau})$, the symmetry breaking effects using the model of Faessler *et al.* [58] increases the magnitude of $\overline{P}_P(E_{\bar{\nu}_\tau})$ while the model of Schlumpf [57] decreases the magnitude of $\overline{P}_P(E_{\bar{\nu}_\tau})$ by about 25% in the entire range of $E_{\bar{\nu}_\tau}$.

C. Implications of lepton flavor universality in neutrino scattering

The lepton flavor universality in the $e - \mu$ sector was proposed long time back in 1947 by Pontecorvo [85] and has been established phenomenologically by studying the weak processes of μ decay, μ^- capture and e^- capture from

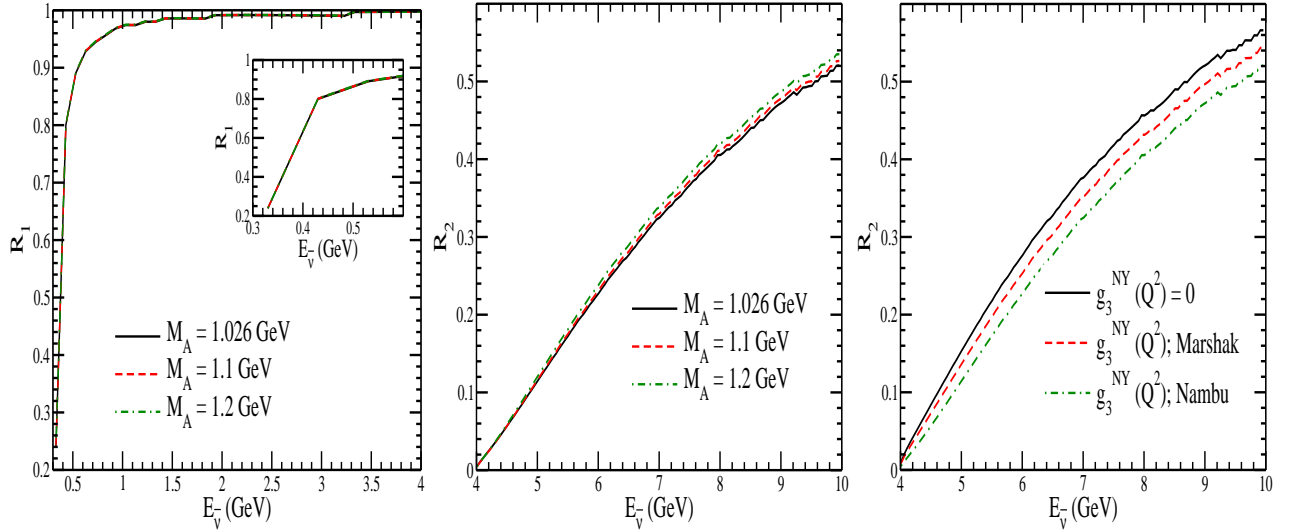


FIG. 15: R_1 as a function of $E_{\bar{\nu}}$ (left panel) with $M_A = 1.026$ GeV (solid line), $M_A = 1.1$ GeV (dashed line) and $M_A = 1.2$ GeV (dashed-dotted line). R_2 as a function of $E_{\bar{\nu}}$ (middle panel) with $M_A = 1.026$ GeV (solid line), $M_A = 1.1$ GeV (dashed line) and $M_A = 1.2$ GeV (dashed-dotted line). R_2 as a function of $E_{\bar{\nu}}$ (right panel) with $g_3^{NY}(Q^2) = 0$ (solid line), the parameterization of $g_3^{NY}(Q^2)$ by Marshak *et al.* [60] (dashed line) and by Nambu [73] (dashed-dotted line).

nucleons and nuclei [86]. After the discovery of τ lepton and the analyses of its leptonic and semileptonic decays, the principle of lepton flavor universality was extended to the $e - \mu - \tau$ sector. As mentioned in the introduction in Section I, recently there has been considerable work in studying the implications of lepton flavor universality in weak interactions in the $e - \mu - \tau$ sector, which have focused mainly on the decay processes [30–42]. While there has been very little work on the study of lepton flavor universality in the scattering processes induced by ν_e , ν_μ and ν_τ . Only two groups have investigated the implications of lepton flavor universality in the $e - \mu$ sector by studying the quasielastic scattering induced by ν_e ($\bar{\nu}_e$) and ν_μ ($\bar{\nu}_\mu$) from the free nucleons [56] and nuclei [55]. They have reported the results comparing the cross sections of quasielastic scattering of ν_e ($\bar{\nu}_e$) and ν_μ ($\bar{\nu}_\mu$) with free nucleons [56] and with nuclear targets [55] induced by the $\Delta S = 0$ weak charged current reactions. In Ref. [56], Day and McFarland have assumed the LFU and studied the differences in the electron and muon production cross section arising due to the lepton mass effect and other effects that depend upon the lepton mass like the radiative corrections, the pseudoscalar form factor as well as the form factors associated with the second class currents. In Ref. [55], Akbar *et al.* have studied these differences in the neutrino-nucleus cross sections including the nuclear medium effects, which are important in the intermediate energy region where most of the present neutrino experiments are being done.

In this section, we study the implications of LFU in the $\Delta S = 1$ sector of antineutrino scattering, and compare the total cross sections for e , μ and τ productions in the quasielastic scattering of $\bar{\nu}_e$, $\bar{\nu}_\mu$ and $\bar{\nu}_\tau$ from the nucleons induced by the weak charged currents. Specifically, we study the ratios of the total cross sections R_1 and R_2 , defined as:

$$R_1 = \frac{\sigma(\bar{\nu}_\mu + p \longrightarrow \mu^+ + \Lambda)}{\sigma(\bar{\nu}_e + p \longrightarrow e^+ + \Lambda)}, \quad (52)$$

$$R_2 = \frac{2\sigma(\bar{\nu}_\tau + p \longrightarrow \tau^+ + \Lambda)}{\sigma(\bar{\nu}_\mu + p \longrightarrow \mu^+ + \Lambda) + \sigma(\bar{\nu}_e + p \longrightarrow e^+ + \Lambda)}, \quad (53)$$

as a function of antineutrino energy $E_{\bar{\nu}}$ and investigate the effect of axial dipole mass M_A and the pseudoscalar form factor $g_3^{NY}(Q^2)$ assuming the SU(3) symmetry. The numerical results are calculated by taking $M_A = 1.026$ GeV and the parameterization of $g_3^{NY}(Q^2)$ by Nambu, unless stated otherwise, and presented in Fig. 15. We have also studied the effect of changing the vector form factors as well as the effect of SU(3) symmetry breaking. These effects are found to be quantitatively very small on $R_1(E_{\bar{\nu}})$ and $R_2(E_{\bar{\nu}})$, and are not presented here.

We see from Fig. 15 that

- (i) the ratios $R_1(E_{\bar{\nu}})$ (Eq. (52)) and $R_2(E_{\bar{\nu}})$ (Eq. (53)) have very little dependence on the choice of M_A , which is almost negligible in the case of $R_1(E_{\bar{\nu}})$. It may be noticed that in the kinematic region of τ production *i.e.*, $E_{\bar{\nu}} \simeq 4$ GeV, the ratio $R_1(E_{\bar{\nu}})$ is almost unity. While in the case of $R_2(E_{\bar{\nu}})$, the ratio is highly suppressed due

to the threshold effects and becomes more than 0.5, only for $E_{\bar{\nu}} > 10$ GeV. Thus, any deviation of $R_1(E_{\bar{\nu}})$ and $R_2(E_{\bar{\nu}})$ from the values shown in Fig. 15, would be a possible signal for the violation of LFU.

- (ii) the ratio $R_2(E_{\bar{\nu}})$ has some dependence on the choice of the pseudoscalar form factor $g_3^{NY}(Q^2)$. If we take $g_3^{NY}(Q^2) = 0$ or the parameterization of $g_3^{NY}(Q^2)$ given by Marshak *et al.* [60], the value of $R_2(E_{\bar{\nu}})$ increases as compared to the value obtained by using the parameterization of $g_3^{NY}(Q^2)$ given by Nambu [73]. For example, at $E_{\bar{\nu}} = 10$ GeV, when we compare the results obtained with $g_3^{NY}(Q^2)$ using the parameterization of Marshak *et al.* [60], the value of $R_2(E_{\bar{\nu}})$ increases by 5%, which becomes 18% at $E_{\bar{\nu}} = 5$ GeV, from the results using $g_3^{NY}(Q^2)$ from the results obtained using $g_3^{NY}(Q^2)$ parameterized by Marshak *et al.* [60]. Therefore, an experimental determination of $R_2(E_{\bar{\nu}})$ with a precision of 20% or higher would be able to show any evidence of the violation of LFU in the $e - \mu - \tau$ sector.

V. SUMMARY AND CONCLUSIONS

In this work, we have presented the results for the $|\Delta S| = 1$ hyperon production in the quasielastic $\bar{\nu}_\tau$ -nucleon scattering and obtained the differential ($\frac{d\sigma}{dQ^2}$) and total (σ) scattering cross sections as well as the longitudinal (P_L) and perpendicular (P_P) components of the polarized τ^+ lepton produced in these reactions. We studied theoretical uncertainties arising due to the use of different vector, axial vector and pseudoscalar form factors as well as the effect of SU(3) symmetry breaking on these observables.

Our observations are the following:

- (i) In the case of Λ production, the total cross section as well as the average polarizations increases with increase in M_A at low antineutrino energies, say at $E_{\bar{\nu}_\tau} = 5$ GeV. However, with the increase in $E_{\bar{\nu}_\tau}$, σ further increases with M_A while $\overline{P}_{L,P}(E_{\bar{\nu}_\tau})$ saturates with increase in M_A . Moreover, in the case of Σ^- production, the results for σ as well as $\overline{P}_{L,P}(E_{\bar{\nu}_\tau})$ are qualitatively similar to the results obtained for Λ production.
- (ii) There is not much effect of SU(3) symmetry breaking on σ for both Λ and Σ^- productions. However, we observe some dependence of the symmetry breaking effect on $\overline{P}_{L,P}(E_{\bar{\nu}_\tau})$, which are qualitatively different for Λ and Σ^- productions.
- (iii) In the case of Λ production, at low $\bar{\nu}_\tau$ energies, specifically near the threshold energy, the effect of the different parameterizations of vector form factors on $\frac{d\sigma}{dQ^2}$, $P_L(Q^2)$ and $P_P(Q^2)$ distributions is large, which decreases with the increase in $E_{\bar{\nu}_\tau}$. However, in the case of Σ^- production, $\frac{d\sigma}{dQ^2}$ shows appreciable dependence on the different parameterizations of the vector form factors for all values of $E_{\bar{\nu}_\tau}$, while $P_L(Q^2)$ and $P_P(Q^2)$ distributions are quite sensitive to the choice of the vector form factors.
- (iv) The effect of variation in the axial dipole mass M_A on $\frac{d\sigma}{dQ^2}$, $P_L(Q^2)$ and $P_P(Q^2)$, when Λ is produced in the final state, is significant at low $E_{\bar{\nu}_\tau}$, which decreases with the increase in $E_{\bar{\nu}_\tau}$ for Q^2 and $P_L(Q^2)$ distributions but for $P_P(Q^2)$ distribution still remains significantly different even at high $\bar{\nu}_\tau$ energies. While there is a large dependence of M_A on $\frac{d\sigma}{dQ^2}$, $P_L(Q^2)$ and $P_P(Q^2)$ at all values of Q^2 and $E_{\bar{\nu}_\tau}$, when Σ^- is produced in the final state.
- (v) In the case of Λ production, the effect of SU(3) symmetry breaking on $\frac{d\sigma}{dQ^2}$ is very small at all values of $E_{\bar{\nu}_\tau}$ and Q^2 while there is a sizeable effect of SU(3) symmetry breaking on $P_L(Q^2)$ and $P_P(Q^2)$. However, in the case of Σ^- production, the effect of SU(3) symmetry breaking on $\frac{d\sigma}{dQ^2}$ is small at low $E_{\bar{\nu}_\tau}$, and increases with the increase in energy. Moreover, different results for the polarization observables are obtained when the SU(3) symmetry breaking using the prescriptions by Schlumpf [57] and Faessler *et al.* [58] are taken into account.
- (vi) We have also tested the lepton flavor universality in the antineutrino induced Λ production by calculating the ratios (given in Eqs. (52) and (53)) of the total cross sections in the $e - \mu$ and $e - \mu - \tau$ sectors. We find that there is no dependence of M_A or the SU(3) symmetry breaking on R_1 . However, R_2 shows some dependence on the choice of M_A as well as to the different parameterizations of the pseudoscalar form factor. Thus, the experimental observation of $R_2(E_{\bar{\nu}})$ with a precision of 20% or higher would be able to show any evidence of the violation of LFU in the $e - \mu - \tau$ sector.

Acknowledgment

A. F. and M. S. A. are thankful to the Department of Science and Technology (DST), Government of India for providing financial assistance under Grant No. SR/MF/PS-01/2016-AMU.

-
- [1] K. Kodama *et al.* [DONUT Collaboration], Phys. Lett. B **504**, 218 (2001).
 [2] K. Kodama *et al.* [DONuT Collaboration], Phys. Rev. D **78**, 052002 (2008).
 [3] N. Agafonova *et al.* [OPERA Collaboration], Phys. Rev. D **89**, 051102 (2014).
 [4] N. Agafonova *et al.* [OPERA Collaboration], Phys. Rev. Lett. **115**, 121802 (2015).
 [5] N. Agafonova *et al.* [OPERA Collaboration], Phys. Rev. Lett. **120**, 211801 (2018).
 [6] Z. Li *et al.* [Super-Kamiokande Collaboration], Phys. Rev. D **98**, 052006 (2018).
 [7] K. Abe *et al.* [Super-Kamiokande Collaboration], Phys. Rev. Lett. **110**, 181802 (2013).
 [8] M. G. Aartsen *et al.* [IceCube Collaboration], Phys. Rev. D **99**, 032007 (2019).
 [9] C. Yoon [SHiP Collaboration], PoS **NuFact2019**, 103 (2020).
 [10] M. Anelli *et al.* [SHiP Collaboration], [arXiv:1504.04956 [physics.ins-det]].
 [11] S. Alekhin *et al.*, Rept. Prog. Phys. **79**, 124201 (2016).
 [12] S. Aoki *et al.* [DsTau Collaboration], JHEP **2001**, 033 (2020).
 [13] P. Machado, H. Schulz and J. Turner, [arXiv:2007.00015 [hep-ph]].
 [14] J. Strait *et al.* [DUNE Collaboration], [arXiv:1601.05823 [physics.ins-det]].
 [15] B. Abi *et al.* [DUNE Collaboration], [arXiv:1807.10340 [physics.ins-det]].
 [16] H. Abreu *et al.* [FASER Collaboration], [arXiv:2001.03073 [physics.ins-det]].
 [17] A. Fatima, M. Sajjad Athar and S. K. Singh, Phys. Rev. D **102**, 113009 (2020).
 [18] K. S. Kuzmin, V. V. Lyubushkin and V. A. Naumov, Mod. Phys. Lett. A **19**, 2815 (2004), [Phys. Part. Nucl. **35**, S133 (2004)].
 [19] K. S. Kuzmin, V. V. Lyubushkin and V. A. Naumov, Mod. Phys. Lett. A **19**, 2919 (2004).
 [20] K. Hagiwara, K. Mawatari and H. Yokoya, Nucl. Phys. B **668**, 364-384 (2003).
 [21] K. Hagiwara, K. Mawatari and H. Yokoya, Nucl. Phys. Proc. Suppl. **139**, 140 (2005).
 [22] K. Hagiwara, K. Mawatari and H. Yokoya, Phys. Lett. B **591**, 113-118 (2004).
 [23] J. E. Sobczyk, N. Rocco and J. Nieves, Phys. Rev. C **100**, 035501 (2019).
 [24] M. Valverde, J. E. Amaro, J. Nieves and C. Maieron, Phys. Lett. B **642**, 218-226 (2006).
 [25] A. Fatima, M. Sajjad Athar and S. K. Singh, Eur. Phys. J. A **54**, 95 (2018).
 [26] A. Fatima, M. Sajjad Athar and S. K. Singh, Phys. Rev. D **98**, 033005 (2018).
 [27] A. Fatima, M. Sajjad Athar and S. K. Singh, Front. in Phys. **7**, 13 (2019).
 [28] A. Fatima, M. Sajjad Athar and S. K. Singh, doi:10.1140/epjs/s11734-021-00272-0 [arXiv:2106.14590 [hep-ph]].
 [29] G. Aad *et al.* [ATLAS Collaboration], Nature Phys. **17**, 813 (2021).
 [30] S. F. Zhang [BESIII Collaboration], [arXiv:1906.08912 [hep-ex]].
 [31] Y. H. Yang [BESIII Collaboration], [arXiv:1812.00320 [hep-ex]].
 [32] R. Fleischer, R. Jaarsma and G. Koole, Eur. Phys. J. C **80**, 153 (2020).
 [33] M. Golz, PoS **CHARM2020**, 051 (2021).
 [34] M. Ablikim *et al.* [BESIII Collaboration], Phys. Rev. Lett. **127**, 121802 (2021).
 [35] M. Ablikim *et al.* [BESIII Collaboration], Phys. Rev. Lett. **122**, 011804 (2019).
 [36] G. Mezzadri [BESIII Collaboration], PoS **BEAUTY2018**, 025 (2018).
 [37] S. Bifani, S. Descotes-Genon, A. Romero Vidal and M. H. Schune, J. Phys. G **46**, 023001 (2019).
 [38] J. Albrecht, D. van Dyk and C. Langenbruch, Prog. Part. Nucl. Phys. **120**, 103885 (2021).
 [39] R. Aaij *et al.* [LHCb Collaboration], [arXiv:2103.11769 [hep-ex]].
 [40] P. de Simone [LHCb Collaboration], EPJ Web Conf. **234**, 01004 (2020).
 [41] G. Caria *et al.* [Belle Collaboration], Phys. Rev. Lett. **124**, 161803 (2020).
 [42] S. Celani [LHCb Collaboration], [arXiv:2111.11105 [hep-ex]].
 [43] A. Crivellin and M. Hoferichter, Science **374**, 1051 (2021).
 [44] D. Bryman, V. Cirigliano, A. Crivellin and G. Inguglia, [arXiv:2111.05338 [hep-ph]].
 [45] B. Abi *et al.* [Muon g-2 Collaboration], Phys. Rev. Lett. **126**, 141801 (2021).
 [46] A. M. Coutinho, A. Crivellin and C. A. Manzari, Phys. Rev. Lett. **125**, 071802 (2020).
 [47] A. M. Sirunyan *et al.* [CMS Collaboration], JHEP **07**, 208 (2021).
 [48] L. Allwicher, G. Isidori and N. Selimovic, [arXiv:2109.03833 [hep-ph]].
 [49] A. Crivellin, M. Hoferichter, M. Kirk, C. A. Manzari and L. Schnell, JHEP **10**, 221 (2021).
 [50] D. London and J. Matias, doi:10.1146/annurev-nucl-102020-090209 [arXiv:2110.13270 [hep-ph]].
 [51] L. Zhang, X. W. Kang, X. H. Guo, L. Y. Dai, T. Luo and C. Wang, JHEP **02**, 179 (2021).
 [52] D. Bećirević, F. Jaffredo, A. Peñuelas and O. Sumensari, JHEP **05**, 175 (2021).
 [53] X. Leng, X. L. Mu, Z. T. Zou and Y. Li, Chin. Phys. C **45**, 063107 (2021).
 [54] S. Zhang [BESIII Collaboration], SciPost Phys. Proc. **1**, 016 (2019).

- [55] F. Akbar, M. Rafi Alam, M. Sajjad Athar, S. Chauhan, S. K. Singh and F. Zaidi, *Int. J. Mod. Phys. E* **24**, 1550079 (2015).
- [56] M. Day and K. S. McFarland, *Phys. Rev. D* **86**, 053003 (2012).
- [57] F. Schlumpf, *Phys. Rev. D* **51**, 2262 (1995).
- [58] A. Faessler, T. Gutsche, B. R. Holstein, M. A. Ivanov, J. G. Korner and V. E. Lyubovitskij, *Phys. Rev. D* **78**, 094005 (2008).
- [59] X. G. He, J. Tandean and G. Valencia, *JHEP* **07**, 022 (2019).
- [60] R. E. Marshak, Riazuddin, C. P. Ryan, *Theory of Weak Interactions in Particle Physics* (Wiley-Interscience, 1969).
- [61] A. Pais, *Annals Phys.* **63**, 361 (1971).
- [62] C. H. Llewellyn Smith, *Phys. Rept.* **3**, 261 (1972).
- [63] R. Bradford, A. Bodek, H. Budd and J. Arrington, *Nucl. Phys. (Proc. Suppl.)* **159** 127 (2006).
- [64] P. E. Bosted, *Phys. Rev. C* **51**, 409 (1995).
- [65] H. Budd, A. Bodek and J. Arrington, *Nucl. Phys. (Proc. Suppl.)* **139**, 90 (2005).
- [66] W. M. Alberico *et al.*, *Phys. Rev. C* **79**, 065204 (2009).
- [67] J. J. Kelly, *Phys. Rev. C* **70**, 068202 (2004).
- [68] S. Galster *et al.*, *Nucl. Phys. B* **32**, 221 (1971).
- [69] S. Platchkov *et al.*, *Nucl. Phys. A* **510**, 740 (1990).
- [70] V. Punjabi, C. F. Perdrisat, M. K. Jones, E. J. Brash and C. E. Carlson, *Eur. Phys. J. A* **51**, 79 (2015).
- [71] N. Cabibbo, E. C. Swallow, R. Winston, *Annu. Rev. Nucl. Part. Sci.* **53**, 39 (2003).
- [72] V. Bernard, L. Elouadrhiri, U. G. Meissner, *J. Phys. G* **28**, R1 (2002).
- [73] Y. Nambu, *Phys. Rev. Lett.* **4**, 380 (1960).
- [74] R. M. Wang, M. Z. Yang, H. B. Li and X. D. Cheng, *Phys. Rev. D* **100**, no.7, 076008 (2019).
- [75] P. E. Shanahan, A. N. Cooke, R. Horsley, Y. Nakamura, P. E. L. Rakow, G. Schierholz, A. W. Thomas, R. D. Young and J. M. Zanotti, *Phys. Rev. D* **92**, 074029 (2015).
- [76] G. S. Yang and H. C. Kim, *Phys. Rev. C* **92**, 035206 (2015).
- [77] D. Becirevic, D. Guadagnoli, G. Isidori, V. Lubicz, G. Martinelli, F. Mescia, M. Papinutto, S. Simula, C. Tarantino and G. Villadoro, *Eur. Phys. J. A* **24S1**, 69 (2005).
- [78] A. Lacour, B. Kubis and U. G. Meissner, *JHEP* **10**, 083 (2007).
- [79] T. N. Pham, *Phys. Rev. D* **87**, 016002 (2013).
- [80] T. N. Pham, *Nucl. Part. Phys. Proc.* **258**, 102 (2015).
- [81] T. Ledwig, J. Martin Camalich, L. S. Geng and M. J. Vicente Vacas, *Phys. Rev. D* **90**, 054502 (2014).
- [82] H. M. Chang, M. González-Alonso and J. Martin Camalich, *Phys. Rev. Lett.* **114**, 161802 (2015).
- [83] M. Ademollo and R. Gatto, *Phys. Rev. Lett.* **13**, 264 (1964).
- [84] S. M. Bilenky, *Basics of Introduction to Feynman Diagrams and Electroweak Interactions Physics* (Editions Frontieres, Gif-sur-Yvette Cedex, 1994).
- [85] B. Pontecorvo, *Phys. Rev.* **72**, 246 (1947).
- [86] M. Sajjad Athar and S. K. Singh, *The Physics of Neutrino Interactions* (Cambridge University Press, Cambridge, England, 2020).